

Background Noise Reduction and Signal Reconstruction for  
Airborne Acoustic Emission of a Machining Process



Author

TAYYAB ZAFAR

NUST201362510MCEME35513F

Supervisor

DR. KHURRAM KAMAL

DEPARTMENT OF MECHATRONICS ENGINEERING  
COLLEGE OF ELECTRICAL & MECHANICAL ENGINEERING  
NATIONAL UNIVERSITY OF SCIENCES AND TECHNOLOGY  
ISLAMABAD  
JULY, 2015

Background Noise Reduction and Signal Reconstruction for  
Airborne Acoustic Emission of a Machining Process

Author

TAYYAB ZAFAR

NUST201362510MCEME35513F

MS-78

A thesis submitted in partial fulfillment of the requirements for the degree of  
MS Mechatronics Engineering

Thesis Supervisor:

DR. KHURRAM KAMAL

Thesis Supervisor's Signature: \_\_\_\_\_

DEPARTMENT OF MECHATRONICS ENGINEERING  
COLLEGE OF ELECTRICAL & MECHANICAL ENGINEERING  
NATIONAL UNIVERSITY OF SCIENCES AND TECHNOLOGY,  
ISLAMABAD  
JULY, 2015

## **Declaration**

I certify that this research work titled “*Background Noise Reduction and Signal Reconstruction for Airborne Acoustic Emission of a Machining Process*” is my own work. The work has not been presented elsewhere for assessment. The material that has been used from other sources it has been properly acknowledged / referred.

Signature of Student

Tayyab Zafar

NUST201362510MCEME35513F

## **Language Correctness Certificate**

This thesis has been read by an English expert and is free of typing, syntax, semantic, grammatical and spelling mistakes. Thesis is also according to the format given by the university.

Signature of Student

Tayyab Zafar

NUST201362510MCEME35513F

Signature of Supervisor

Dr. Khurram Kamal

## **Copyright Statement**

- Copyright in text of this thesis rests with the student author. Copies (by any process) either in full, or of extracts, may be made only in accordance with instructions given by the author and lodged in the Library of NUST College of E&ME. Details may be obtained by the Librarian. This page must form part of any such copies made. Further copies (by any process) may not be made without the permission (in writing) of the author.
- The ownership of any intellectual property rights which may be described in this thesis is vested in NUST College of E&ME, subject to any prior agreement to the contrary, and may not be made available for use by third parties without the written permission of the College of E&ME, which will prescribe the terms and conditions of any such agreement.
- Further information on the conditions under which disclosures and exploitation may take place is available from the Library of NUST College of E&ME, Rawalpindi.

## **Acknowledgements**

First and foremost, I thank Allah (SWT) for endowing me with health, patience, and knowledge to complete this work. Without health and facility given by Allah SWT unlikely I cannot done the thesis successfully. Whosoever helped me throughout the course of my thesis, whether my parents or any other individual was Allah's will, so indeed none be worthy of praise but Allah.

I am grateful to my parents and siblings who always helped and supported me during my education. Without them, I would never be able to complete this thesis. I am profusely thankful to my beloved parents for everything they have done for me.

I express my deepest gratitude to my supervisor Dr. Khurram Kamal for his always encouraging behavior. Before him, research was a boring and tough subject for me. He taught me how to conduct research effectively. His dedication to the teaching and research set a new standards for me. Throughout the thesis, he was more of a mentor than a supervisor to me.

I would also like to express my special thanks of gratitude to Dr. Javaid Iqbal, Dr. Kunwar Faraz Ahmad and Dr. Zakaullah Sheikh for being on my thesis guidance and evaluation committee. I am especially thankful to them for their support and cooperation.

I would like to express my gratitude to all the friends specially (soon-to-be Dr.) Nasir Rashid who have rendered valuable assistance to my study.

I acknowledge, the effort being made by the department in providing me all the facilities to attain the highest standards of excellence & the efforts of the faculty members in transferring their precious knowledge to us.

*Dedicated to my exceptional parents and adored siblingsto express myunspoken love*

*"You don't really understand human nature unless you know why a child on a merry-go-round will wave at his parents every time around, and why his parents will always wave back" ~William D. Tammeus*

## ABSTRACT

Intelligent machining centers have become important part of manufacturing systems because of increased demand of the productivity. Tool Condition Monitoring is an integral part of these systems. Acoustic emission from machining process is an important indicator of tool health. Acoustic emission for a metal cutting process can be divided into two categories, structure-born acoustic emission and airborne acoustic emission. Structure-borne acoustic emission needs high processing power whereas, background noise is a great challenge in case of airborne acoustic emission. Reducing the background noise may help in developing a low-cost system. Four different machine algorithms, have been used as adaptive filters in order to reduce the background noise. These algorithms include feedforward neural network trained with Levenberg-Marquardt algorithm, self-organizing maps, K-mean clustering algorithm and Particle Swarm Optimization (PSO). Acoustic signals from four different machines in background are acquired and are introduced to a machining signal at different RPMs and feed-rates at a constant depth of cut. The four machines are 3-axis milling machine, 4-axis mini-milling machine, a variable speed DC motor and a grinding machine. These background noise signals are filtered through the proposed algorithms. Backpropagation neural network shows the better performance for the filtering while the other algorithms work only for dominant noise. The average accuracy of the backpropagation neural network is found to be 75.82%. The filtered signal is reconstructed using Auto Regressive Moving Average (ARMA) technique. An average increase of 71.3% in SNR is found before and after signal reconstruction. ARMA shows a promising results for signal reconstruction for machining process.

# Table of Contents

Declaration .....	i
Language Correctness Certificate .....	ii
Copyright Statement .....	iii
Acknowledgements .....	iv
ABSTRACT .....	vi
Table of Contents .....	vii
List of figures .....	ix
List of Tables .....	x
1. INTRODUCTION .....	1
1.1. Introduction To Thesis .....	1
1.2. Summary .....	3
2. LITERATURE REVIEW .....	4
2.1. Techniques in tool condition monitoring .....	4
2.2. Background noise reduction methods .....	13
2.3. Signal reconstruction techniques.....	17
2.4. Thesis aims and objectives.....	18
2.5. Summary .....	19
3. TOOLS AND TECHNIQUES.....	20
3.1. Adaptive filters.....	20
3.2. Signal reconstruction.....	26
3.2.1. Identification of model order:.....	27
3.2.2. Estimation of model coefficients .....	30
3.2.3. Proposed algorithm for signal reconstruction .....	31
3.3. Summary .....	34
4. EXPERIMENTATION.....	35
4.1. Experimental setup.....	35
4.2. Summary .....	42
5. RESULTS AND DISCUSSION.....	42
5.1. Adaptive filtering .....	43
5.2. Signal reconstruction.....	53
5.3. Summary .....	57

6. CHALLENGES .....	58
6.1. Summary .....	59
7. CONCLUSION AND FUTURE WORK .....	60
7.1. Summary .....	63
REFERENCES .....	64

## List of figures

<b>Figure 2.1.</b> Algorithm principle [8].....	5
<b>Figure 2.2</b> System schematic [11].....	6
<b>Figure 2.3</b> Vibration signals at different tool conditions [12].....	7
<b>Figure 2.4</b> Heat generating regions [14] .....	8
<b>Figure 2.5</b> Chip formation at different cutting conditions [17].....	11
<b>Figure 2.6</b> Signal Separation [23] .....	14
<b>Figure 2.7</b> (a) Noise signal (b) machine signal (c) Noise free signal [26].....	16
<b>Figure 3.1</b> Feed Forward Neural Network Structure [32].....	21
<b>Figure 3.2</b> Self-organizing map neural network structure [33].....	23
<b>Figure 3.3</b> Autocorrelation function [38].....	28
<b>Figure 3.4</b> Partial Autocorrelation function [39] .....	29
<b>Figure 3.5</b> ACF test for stationary and non-stationary series [37].....	29
<b>Figure 3.6</b> ARMA based reconstruction algorithm flowchart .....	32
<b>Figure 3.7</b> Flowchart of proposed algorithm .....	33
<b>Figure 4.1</b> Experimental setup .....	35
<b>Figure 4.2</b> Close view of microphone setup .....	36
<b>Figure 4.3</b> (a) Raw acoustic signal (above), (b) RMS level of the signal.....	39
<b>Figure 4.4</b> FFT plot of machining signal .....	39
<b>Figure 4.5</b> Raw acoustic signals of background noise .....	41
<b>Figure 4.6</b> (a) RMS plot of machines (above), (b) RMS plot of grinding machine (below) .....	41
<b>Figure 5.1</b> Training curve of back-propagation neural network .....	44
<b>Figure 5.2</b> Confusion matrix for machining signal .....	45
<b>Figure 5.3</b> Self-Organizing Map Neural Network clusters for training data .....	45
<b>Figure 5.4</b> SOM response for machining signal .....	46
<b>Figure 5.5</b> K-Means training data clustering .....	47
<b>Figure 5.6</b> K-Means clustering for machining data .....	47
<b>Figure 5.7</b> Training curve of PSO neural network.....	49
<b>Figure 5.8</b> Confusion matrix for PSO testing .....	49
<b>Figure 5.9</b> Noise introduction (above) and RMS level of the same signal (below).....	51
<b>Figure 5.10</b> FFT Plot of signal before and after addition of noise.....	52
<b>Figure 5.11</b> Signal filtration using back-propagation neural network .....	53
<b>Figure 5.12</b> ACF plot .....	54
<b>Figure 5.13</b> PACF Plot.....	54
<b>Figure 5.14</b> Reconstructed Signal .....	55

## List of Tables

<b>Table 2-1</b> Comparison of various techniques.....	12
<b>Table 4-1</b> Various features of acquired signals.....	37
<b>Table 4-2</b> Background machine distance measures .....	40
<b>Table 5-1</b> Parameter values for PSO algorithm .....	48
<b>Table 5-2</b> Results Summary .....	50
<b>Table 5-3</b> Variance value at different order of difference.....	53
<b>Table 5-4</b> Estimated coefficients values.....	54
<b>Table 5-5</b> Results for real scenarios .....	56

# 1. INTRODUCTION

This chapter presents an introduction to tool condition monitoring using various methods with focusing on acoustic emission, research aims, scope of the research, motivation lying behind the thesis and importance of tool condition monitoring.

## 1.1. Introduction To Thesis

Manufacturing sector of a country plays a major role in country's economic development. According to Worldbank, in 2011, the total value of manufacturing industry of the world is 11.185 trillion U.S dollars[1]. With the increase in the production demand, maintenance of machines becomes more and more important to increase the machine life as well as to increase production. Breakdown maintenance not only increases the productivity cost but also wastes time. According to an estimate, the breakdown time of a machine can be up to 20% of the machining time[2]. To reduce the production time as well as the manufacturing cost, predictive maintenance has been introduced. Early diagnostic of tool condition not only save time but also increases productivity. Currently, 15% of the total production time is used to carry out the predictive maintenance while the manufacturers wants this time to increase it by 33% [3]. Intelligent machining centers have become important part of manufacturing systems. Tool Condition Monitoring is one of the major research area in these centers. Using predictive maintenance, an effective tool condition monitoring system can save 30-35% of machining time[4].

Various methods have been proposed by researchers to monitor the tool health. Generally, these methods can be classified into two categories, direct methods and indirect methods. Direct methods are based on the physical geometry of tool that directly indicate the tool condition. These techniques may involve optics, electrical resistance and radioactive to the measure of tool health. The main advantage of these methods is the accuracy in predicting tool health due to direct measurement from the tool geometry. However, these methods require to stop the machine which not only interrupts the production but may also increases the production cost. Indirect methods are based on the signals that may generate from machining process. These methods may

involve vibration signal from the tool, vision, sensor fusion based systems, acoustic emission, etc., as the measure of tool health. Each technique has its own advantages and disadvantages, however, acoustic emission from the machining process is generally taken as an important indicator of the tool health.

Sudden redistribution of stresses due to crack growth or dislocation in the material structure results in the generation of elastic waves. This quick release of energy from stressed areas of material is known as Acoustic Emission. Acoustic Emission can be divided into two categories, structure-borne acoustic emission and air-borne acoustic emission. Structure-borne acoustic emissions are the vibrations that are transferred from tool to tool holder. For a metal cutting process, the characteristic frequency of the emission lies within the range of 500 KHz to 1 MHz (ultrasonic range)[5]. The structure-borne acoustic emission being having ultrasonic frequency range is an environmental noise free technique, however, it requires high computational processing power. Air-borne acoustic emissions are the vibrations that are transferred from cutting edge to surrounding. The air-borne acoustic emission lies within audible range i.e. from 0 Hz to 20 KHz[5]. Relationship between air-borne acoustic emission and tool vibrations is determined by [6]. They found the vibrations from tool holder, along with the cutting insert are the major source of sound generation. The major challenge in implementing air-borne acoustic emission is to have background or environmental noise[7].

To overcome this problem, an adaptive technique based on neural network is proposed. The machining signal could be filtered through traditional filters, however, the traditional filters would fail within the characteristic frequency range. The proposed method adapts itself according to environmental conditions and extracts the machining signal from background noise effectively.

The thesis is organized in following sections. Chapter 2 presents the previous work related to tool condition monitoring techniques, background noise reduction and signal reconstruction methods. Chapter 3 explains the theory behind the chosen methods while chapter 4 and chapter 5 explain the experimental setup and data acquisition, and the results and detailed discussion respectively. Chapter 6 discusses the challenges related to implementation of the proposed technique and future work.

## 1.2. Summary

This chapter describes

- ❖ Manufacturing sector has a major share in country's economy and it needs to improve its productivity. Breakdown maintenance has various problems that leads to production loss. Therefore, there is a need of predictive maintenance.
  
- ❖ Two types of methods are used to monitor tool health; direct methods and indirect methods. Direct methods cannot be applied during runtime of the machine, therefore, indirect methods are preferred in the regard. Various indirect methods have been proposed by researchers. Acoustic emission is taken as most widely used signal.
  
- ❖ Airborne Acoustic emission can provide an important indication to tool health condition. However, background or environmental noise can deteriorate the signal. Therefore, environmental noise must be removed from the signal.

## 2. LITERATURE REVIEW

This chapter provides a discussion on various methods that have been used to monitor tool health. A comparison of discussed technique is also provided in the chapter. Various techniques used to eliminate or reduce environmental noise from the signal are also explained. Lastly, a discussion on signal reconstruction methods using statistical techniques is also included in the chapter.

### 2.1. Techniques in tool condition monitoring

Different researchers proposed different techniques to monitor the tool health. As mentioned earlier, these techniques can generally be divided into two categories, direct methods and indirect methods.

In direct methods, vision based systems are in use to measure the tool condition. There are many advantages of these systems.

1. The system does not contact with the work-piece or tool, therefore, they do not exert any external force on the system.
2. The system is more flexible and cost effective.
3. The system provides 2D information about the process.
4. Both tool imprints and tool geometry can be observed.
5. The system cannot be affected by high frequency forces as in the case of cutting force signals.

Sortino[8] monitor the tool wear using digital image processing technique. He acquired images of cutting edge of tool using a camera having a  $50\times$  magnification factor at  $640\times 480$  resolution. The every pixel in the image had the dimension of  $10\mu\text{m}$ . After image acquisition, he applied a statistical high-pass filter. Once the edges of the image are detected, its neighboring pixels were grouped in sets as shown in figure 2.1.

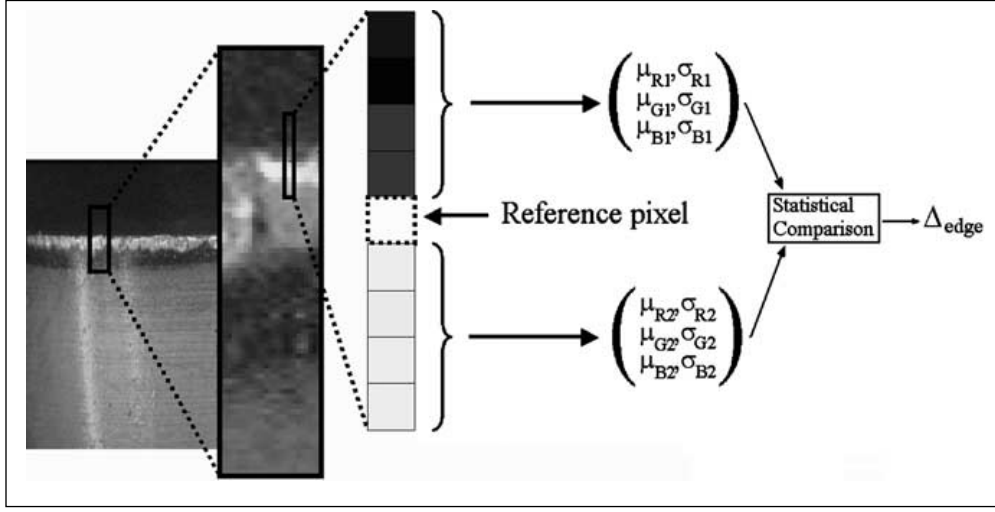


**Figure 2.1.** Algorithm principle[8]

Then  $\Delta_{edge}$  for each basic color is calculated using equation 1 and 2. The value of  $\Delta_{edge}$  can be taken as the probability of the pixel being an edge.

$$\begin{cases} \Delta_{edge}^R = \frac{\mu_{R1} - \mu_{R2}}{\sigma_{R1}^2 - \sigma_{R2}^2} \\ \Delta_{edge}^G = \frac{\mu_{G1} - \mu_{G2}}{\sigma_{G1}^2 - \sigma_{G2}^2} \\ \Delta_{edge}^B = \frac{\mu_{B1} - \mu_{B2}}{\sigma_{B1}^2 - \sigma_{B2}^2} \end{cases} \quad (2.1)$$

$$\Delta_{edge} = \Delta_{edge}^R + \Delta_{edge}^G + \Delta_{edge}^B \quad (2.2)$$

There are some limitations of the proposed technique, e.g., lighting condition should carefully be set to acquire the proper image. There should not be any reflection on the tool during image acquisition as that would produce an edge effect in the image. A review on other image processing techniques is given in [9]. The technique is suitable only for off-line methods and machine has to be stopped to acquire image.

To avoid these issues, indirect methods were introduced by the researchers. Various signals such as cutting force, temperature, vibration from the tool and tool holder, acoustic emission etc., from the machining process can be used to observe the tool condition[10]. These methods can be used online i.e., for real time prediction and they can be used for offline analysis using recorded signals. Xiaoli Li[11]worked on development of a tool condition monitoring system using feed motor current signal. The feed motor drive system was consist of ball screw, cutting tool, tool post, feed motor and feed box etc.

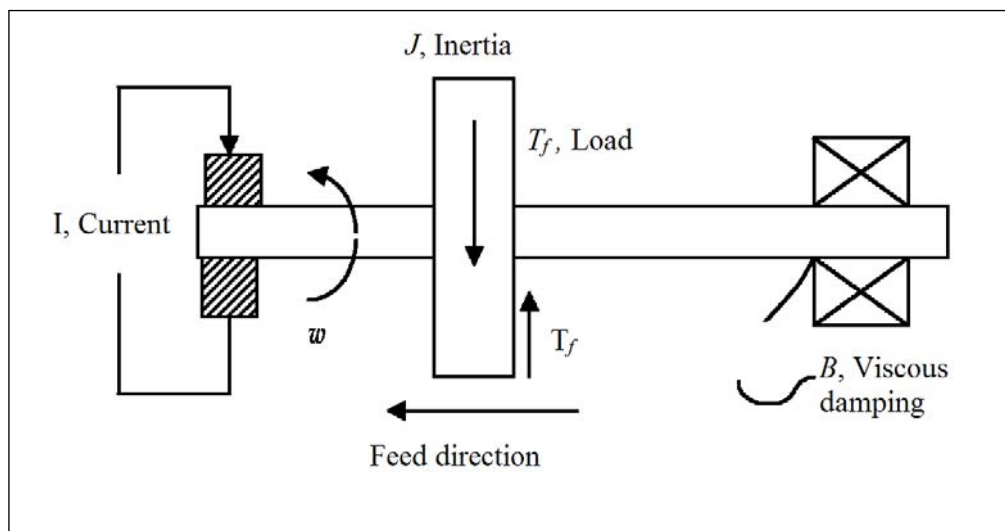


**Figure 2.2** System schematic[11]

The author developed a mathematical model of this system and he was of the view that tool life, based on three different flank wear processes, can be divided into three phases; break-in phase, normal wear phase and catastrophic phase. The AC-feed motor current was recorded through Hall Effect Sensors at different feed-rate, speed and depth of cut. One of the limitation of the described method is that the said system cannot monitor the small cuts because of the small magnitude of the signal.

Ahmed et al.[12] recently developed a vibration signal based system for the purpose. They used piezoelectric signal to convert vibration into electrical signal. Feed-rate, cutting speed and depth

of cut was used as the distinguished features. Only cutting speed was taken as variable while other two features were taken as constant. Work piece material was medium carbon steel while the tool material was uncoated cemented carbide. To acquire the signal, the sensor was mounted on the tool holder in the perpendicular direction to cutting force. The sampling frequency was 200 kHz. The acquired signals were then analyzed using I-kaz method in Matlab. The authors found that with the increase in the tool wear, the amplitude of the vibration signal in the time decreases.

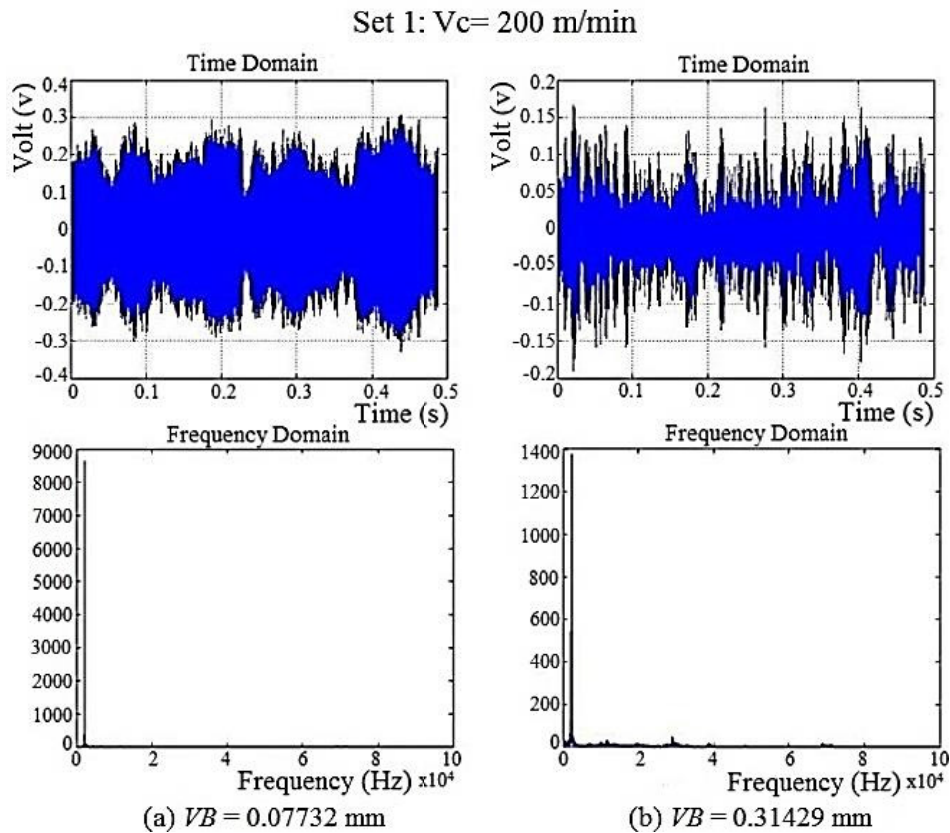


**Figure 2.3** Vibration signals at different tool conditions [12]

Chelladurai et al. [13] monitored the tool condition for high speed turning process using vibration and strain signals. They used the Electric Discharge Machine (EDM) to (artificially) create the tool wear of known properties. A copper rod having flank wear is used as a cathode in EDM to create the wear on cutting tool while the cutting tool made of tungsten carbide material was used

as an anode in the process. Then two accelerometers and two strain gauges were installed on tool to acquire signals. Depth of cut, feed-rate and cutting speed were taken as features in the experiment. These features were used as the input in the backpropagation neural network. The authors found that with increase in the first two parameters, amplitude of acceleration and magnitude of vibration increase. However, with increase in the cutting speed, these signal amplitudes decrease.

During metal cutting process, work done by the tool causes the change in temperature of the tool and work-piece. For a turning process, the temperature changing areas can be divided into three regions; interface between chip and tool, shear zone and, the interface between tool and work-piece. These regions are shown in figure 2.4.

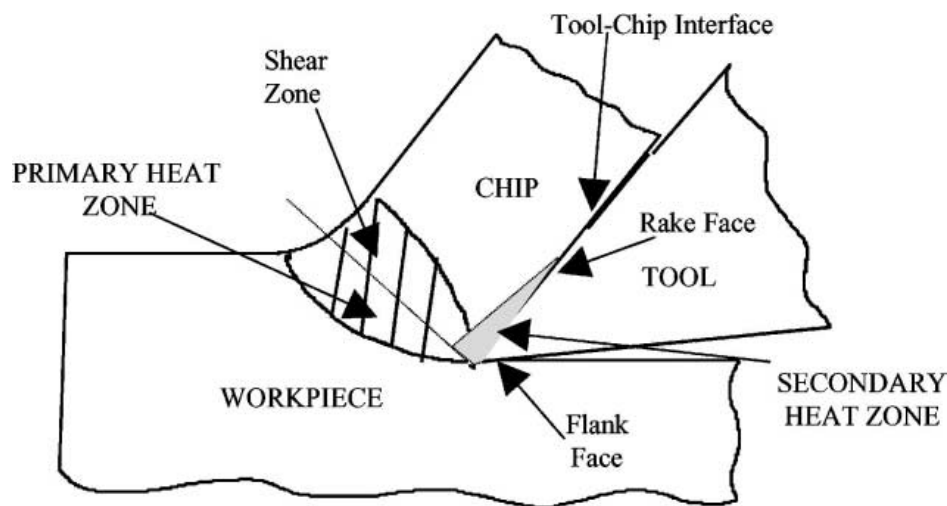


**Figure 2.4** Heat generating regions[14]

O'Sullivan and Cotterell [14] monitor the tool quality using thermal sensing system. The data was acquired through K-types thermocouples, infrared thermal camera to measure temperature. The system also measured cutting force using a dynamometer. An aluminum alloy tube work-piece was used with external diameter of 150mm. Two thermocouples were installed inside the tube. The work-piece was also coated with black paint. The thermal camera was mounted on 0.5m above the work-piece. The authors found that an increase in the cutting speed, resulted in

decrease the cutting force and machine surface temperature. They also found that with increase in the tool wear, amplitudes of the signals also increase.

Combination of all above mentioned signals can be to form a sophisticated tool condition monitoring system. In general, all the signals coming from the various sensors are fed to neural network and tool health is predicted based on signal values. Ghosh et al., [15] estimated average flank wear of a main cutting edge of tool for a milling process.

Several experiments were performed in industrial as well as in lab environment. They used a combination of seven sensors which were cutting force sensor, tool and work-piece vibration measurement sensor, spindle current and voltage sensors, sound pressure level sensor, and AE sensor. Single level segmentation was done to extract the complete lobes that contain machining process information. These lobes were then filtered through a fourth order low pass filter and registered temporarily using a marker signal of cutting force. In order to integrate the different signals, back-propagation neural network was used. The neural network predicts the tool wear.

Segreto et al. [16] used Cutting Force signals (in  $F_x, F_y$  and  $F_z$  direction) , Vibration signals ( $a_x, a_y$  and  $a_z$ ) and Acoustic Emission as input to the neural network. The vibration sensor was mounted on tool holder side; cutting force sensor was installed on the slot between the tool holder and its supported fixture; and acoustic emission sensor was screwed under tool holder head. Separate sampling rates were set for the signals. Four features from the signals were extracted through Linear Predictive Analysis. These feature vectors then combined with all the acquired signal and taken as input to the neural network.

To test the capability of the sensor fusion technique, the authors combine acoustic emission with other signals separately. They found that system prediction is more accurate in case of cutting force and acoustic emission than vibration signal and acoustic emission. However, most accurate results were found when all signals were combined together to predict tool wear. The method has some shortcomings in terms of installing sensors. Moreover, vibration signals can be affected

due to vibrations from other parts of the machine. To avoid the issues, only Acoustic Emission, being a contact-less technique, can be used.

As discussed in the chapter 1, Acoustic Emission can be divided into two types; structure-borne acoustic emission and air-borne acoustic emission. Bhuiyan et al. [17] developed an acoustic emission based system to monitor the tool wear. Several experiments were performed by the authors at different cutting speed, feed-rate and depth of cut. The tool insert was made of TiN coated with carbide while the work-piece was made of mild carbon steel. The acoustic sensor had frequency range of 50kHz to 1MHz through a combination of low and high pass filters. The authors concluded that frequency of Acoustic Emission as well as its RMS can indicate tool health and the type of chip formation can indicate the different cutting conditions.

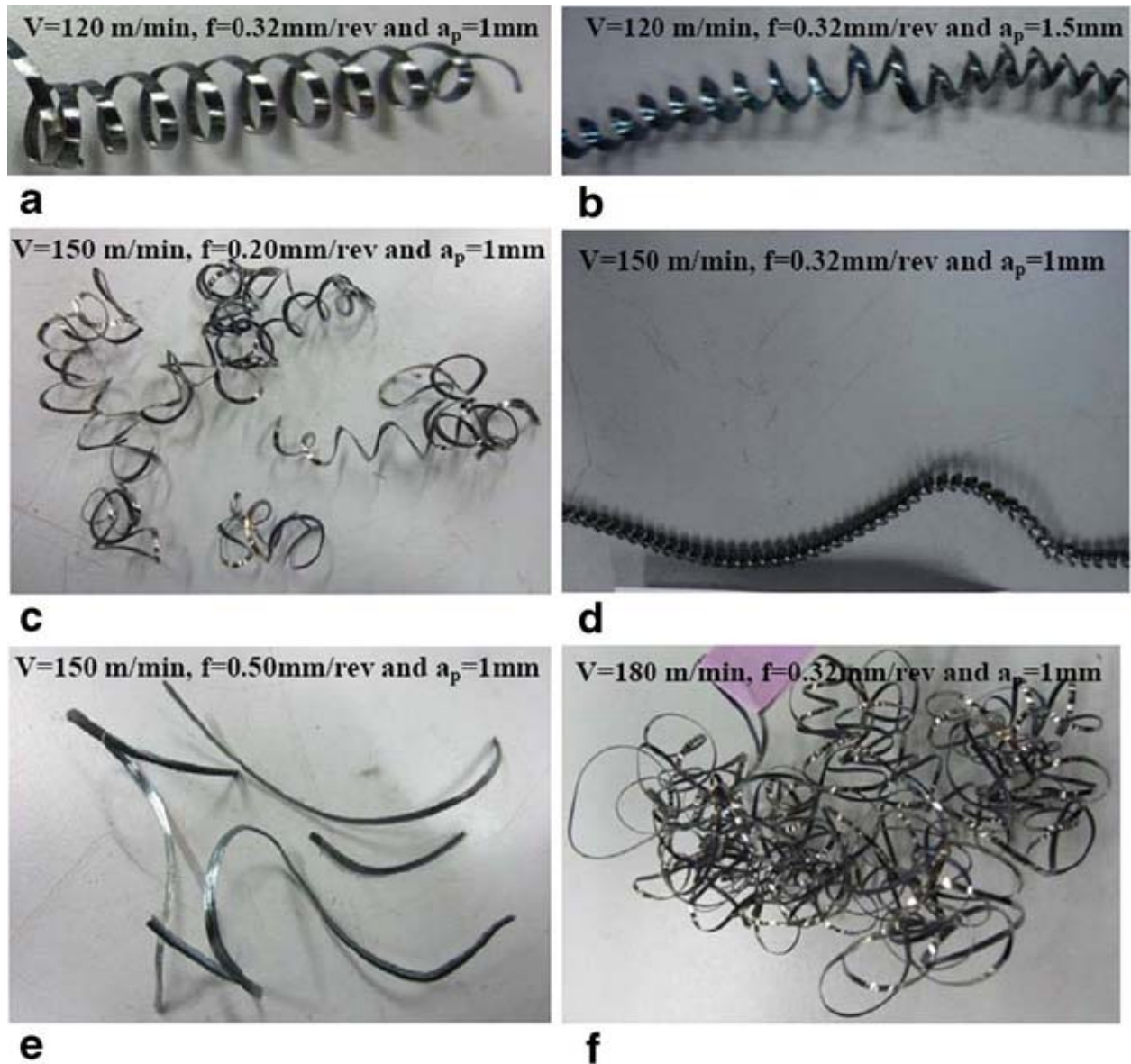


**Figure 2.5** Chip formation at different cutting conditions [17]

Hase et al. [18] found relationship between cutting phenomena and acoustic emission. They also found that chip formation process, chip type and shear angle affect the Acoustic Emission of the process. A review on acoustic emission methods for turning process is given in [19]

As explained earlier, structure-borne Acoustic Emission required high processing and computational power, therefore, Airborne Acoustic Emission can be considered. Airborne Acoustic Emission has frequency range between 0 Hz to 20 kHz. Kopac and Sali [20] developed

tool monitoring system using Airborne Acoustic Emission. They conducted several experiments with different cutting speeds, feed-rates and different amount of wear. The depth of cut was taken as constants in the experiments. The tool insert was made of cermet material without any coating while the work-piece was made of carbon steel Ck15. They found that with increase in the tool wear, the sound intensity between 6 kHz frequency to 20kHz. They concluded that the range depends upon both cutting speed and feed-rate, however the effects of cutting speed are less on the range than feed-rate.

A Hilbert Huang Transform based system was developed by Raja[21] using airborne acoustic emission. They measured the values of RMS amplitude of Intrinsic Mode Function and found that IMF 6,7 and 8 components of the signals change with increase in the amplitude. Another approach to predict remaining life of tool using air-borne acoustic emission can be found in [22].

Comparison of advantages and limitations of above mentioned techniques is summarized in table 1.

**Table 2-1** Comparison of various techniques

Sensing Method	Type	Advantages	Limitations
<b>Vision system</b>	Direct	<ul style="list-style-type: none"> <li>➤ Accurate prediction</li> <li>➤ Low Cost</li> </ul>	<ul style="list-style-type: none"> <li>➤ Off- line method</li> <li>➤ Needs proper Lighting conditions</li> </ul>
<b>Cutting Force Signal</b>	In-direct	<ul style="list-style-type: none"> <li>➤ Reliable</li> </ul>	<ul style="list-style-type: none"> <li>➤ Sensitive to cutting</li> </ul>

			conditions ➤ Only applicable to heavy cuts
<b>Vibration Signal</b>	In-direct	➤ Robust ➤ Free from environmental noise	➤ Sensitive to vibrations from other machine parts, ➤ Sensor installation issue
<b>Temperature Sensing</b>	In-direct	➤ Low cost ➤ Rapid response ➤ Readily available voltage output	➤ May be affected by coolant ➤ Environment
<b>Sensor Fusion</b>	In-direct	➤ Sophisticated system ➤ Real time prediction	➤ Complex ➤ Integrating signals of various tool conditions may itself be a problem
<b>Structure borne Acoustic Emission</b>	In-direct	➤ Reliable, ➤ Highly sensitive	➤ Computationally expensive
<b>Air-borne Acoustic Emission</b>	In-direct	➤ Contact-less technique ➤ Cost effective	➤ Sensitive to environmental noise, ➤ Parallel machining

## 2.2. Background noise reduction methods

One of the major challenge in implementation of the airborne acoustic emission in the industry is environmental noise from the machine surroundings[7]. Many researchers have proposed different methods to de-noise the signal.

Jang and Lee [23] worked on blind source separation using a single channel recording. They developed an algorithm to analyze a signal statistically by employing Maximum Likelihood Method and set of Independent Component Analysis basis function. From the training set, set

of basis function learned a priori and these sets are then used to separate the sources. The authors assumed a signal of two types of generative model observed in the single channel. This is shown in figure 2.7. The algorithm uses maximum a posteriori to find the maximum likelihood. The authors used male and female voices as case study and were of the view that the method can be applied to real world problems. The proposed algorithm has a limitation that it can separate two very distinct sounds and the sound should not be closer to each other.

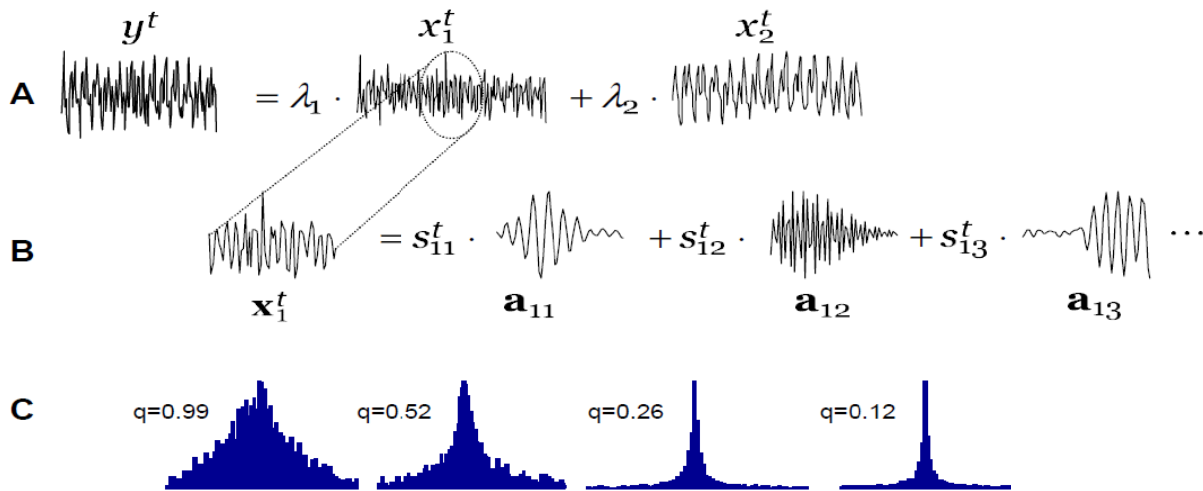
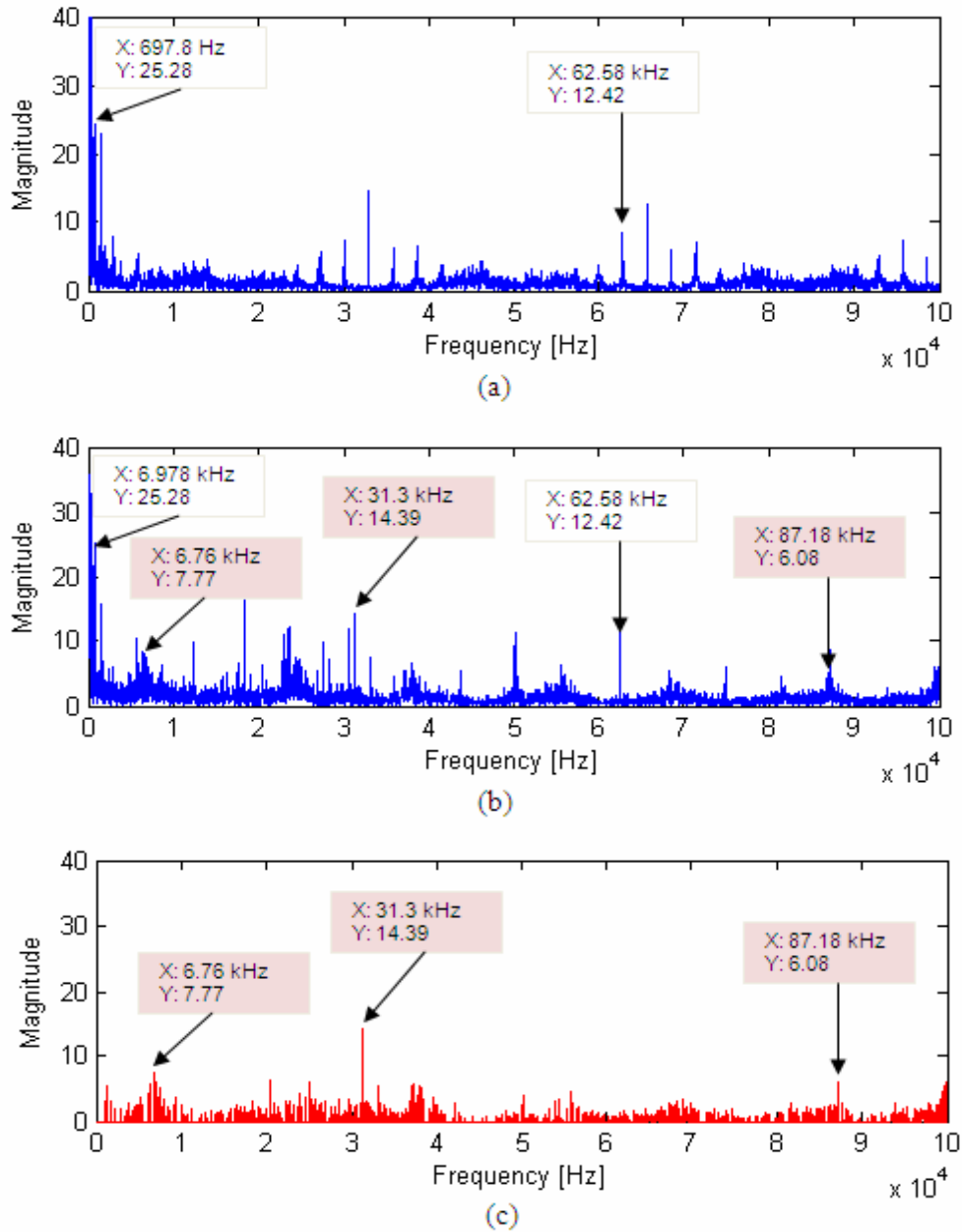


Figure 2.6 Signal Separation[23]

Ruiz-Carcel et al. [24] proposed the spectral kurtosis as a tool to increase the Signal to Noise Ratio of an acoustic emission for roll bearing acoustic emission. A test rig was developed to conduct the experiments. Piezoelectric sensor with operating range of 100 kHz to 1 MHz and sampling rate of 8 MHz was installed on the bearing housing. Acoustic emission was acquired from the rig with rotating speed of motor as 1500 rpm and load applied was 5.3 kN. The major advantage of the technique is automatic selection of band-pass frequency to increase the SNR. Spectral Kurtosis was used to determine the band-pass frequency and FIR filters were used to filter the noise out. The described technique would fail in case if the noise frequency lies within close range of bearing frequency.

Zang et al. [25] proposed an algorithm to remove background noise from the engine signal to improve the signal quality. They used Independent Component Analysis in combination with Radial basis neural network to develop a Volterra Adaptive Noise Cancellation system. They used this system to remove background engine noise from the faulty engine sound. The engine was operating at 1000 RPM and 5000 samples of noise as well as engine signal were acquired at 44100 Hz frequency. The template noise is used to train the RBF neural network and another time series was introduced and predicted the background noise in the signal.

A z-notch filter based technique, to remove the background noise, was introduced by Nuawi et al. [26]. Background noise was removed, from the machine signal by employing z-notch filter and correlating the noise signal with the machining signal. Using a high frequency microphone sensor, Machining signal was acquired during turning operation on a CNC machine. Sounds from other parts of CNC machine such as, motor, hydraulic system, and from its environment were taken as background noise. The sound was recorded without any interaction between the work piece and tool. In order to remove the frequency components of noise from the machining signal, the signal was then passed through a z-notch filter. The limitation of the technique is constant or known frequencies of the noise and it can only be applied for the frequencies which are not close to machining signal frequency.



**Figure 2.7** (a) Noise signal (b) machine signal (c) Noise free signal [26]

In tool health monitoring using vibration sensing, vibrations from other parts of machine may deteriorate the machining vibration signal. Senthilkumar et al. [27] recently developed a system to detect unwanted vibrations in the tool condition monitoring. The signals from three different locations, head stock, lathe bed and compound rest, were acquired using an accelerometer of 100 mV/g sensitivity. Vibrations from other parts of machines were confirmed by the presences of

calculated and measured characteristics frequencies of roller bearing, gear mesh and belt drive in the signal.

### **2.3. Signal reconstruction techniques**

Various signal reconstruction techniques were proposed by the researchers in various fields. Candès et al [28] proposed a signal reconstruction technique using convex optimization technique. The technique extracts the exact signal from the noise using incomplete information of frequency. In the traditional techniques, Fourier coefficients of unobserved frequencies are assumed to be zero, which results in inaccurate signal reconstruction. To overcome this, interpolation between the neighbors can be made. However, this may be a very delicate task due to highly oscillatory nature of the Fourier transforms. The proposed technique tried to find the solution with minimum complexity which they called total variation.

Ukte et al [29] developed an algorithm for signal reconstruction using low resolution noisy measurements. The traditional Wiener filter required the prior knowledge of correlation information about the high and low resolution signal. However, the proposed algorithm needs only the down-sampling rate information to reconstruct a signal. It used Iterative Empirical Mode Decomposition (EMD) interval thresholding based method to decompose and remove the additive white Gaussian noise from the signal. The algorithm then developed the low resolution noisy signals to reconstruct high resolution signals.

Baraldi et al. [30] worked on a signal reconstruction technique based on modified Auto Associative Kernel Regression (AAKR) method for condition monitoring of industrial components. The main aim of the research was to develop a technique with low computation cost, and reconstruction high accuracy. The modification in the traditional AAKR was based on computing the similarity measure. The traditional AAKR method uses Euclidean or Mahalanbis distance as similarity measure, however, the proposed technique introduced a penalty vector which reduced the impact of abnormal or faulty signals. The whole method was

based on the assumption that the probability of occurrence of a fault causing variations on a more number of signals is lower than that of one causing variations on a less number of signals.

Signal analysis using wavelet packet transform for tool condition monitoring was done by Chuangwen et al. [31]. Cutting signals vibrations at different milling wear conditions were recorded. These signals were separated in time-frequency domain by employing multi-resolution wavelet packet transform technique. It was found that resolution of the high frequency band was decreased with the increase in the scale factor. To calculate the energy distribution character of the signal, the authors took a layer of the reconstructed vibration signal energy as energy characteristic vector. Then the recorded vibration signal was breakdown into 3 layers and signal characters were extracted using 8 frequencies and each frequency band signal was extracted using coefficients modeled by wavelet packets.

## **2.4. Thesis aims and objectives**

The scope of the research is quite broad, however, according to level of research and based on the literature review, the thesis aims and objectives can be defined as follows

- I. To devise an adaptive filtering technique in order to eliminate background noise from machining signal of a turning process.
- II. To reconstruct the filtered signal using a time series model
- III. To benchmark the performance of proposed algorithm

## 2.5. Summary

The chapter can be summarized as follows:

- ❖ Direct and Indirect methods have been used in the literature to monitor tool condition. As direct methods have the limitation of offline analysis, therefore indirect methods are preferred.
  
- ❖ Among the indirect methods, various signals such as vibration signal, cutting force signal, sensor fusion, and acoustic emission are used. Each method has its own advantages and limitations. However, mostly vibrations based analysis and acoustic emission are used. Acoustic emission being a low cost and contact-less technique is preferred.
  
- ❖ For the manufacturing process, background noise is taken as a major issue in implementation of airborne acoustic emission, however, parallel machining noise is not addressed in the literature.
  
- ❖ In signal reconstruction methods for the machining process, wavelet analysis is used in the literature. No statistical method for signal reconstruction in the area of tool condition monitoring is cited in the literature.

### **3. TOOLS AND TECHNIQUES**

This chapter explains the techniques used to fulfill the scopes of thesis as well as the background theory related to them. The Chapter is divided into two main sections; explaining the different paradigms of adaptive filters, and statistical time series model to reconstruct the filtered signal.

#### **3.1. Adaptive filters**

Different machine learning techniques are proposed to use as adaptive filters in order to filter the background noise from the machining signal. These techniques include neural network with both supervised and unsupervised learning, clustering technique and optimization algorithms.

Neural networks are computational models which are biologically inspired from human brain. A neural network consists of a number of neurons which are inter-connected individual processing units. Information from system is fed to a neuron using some channels which are known as dendrites. This information or input is then amplified by some amplification factor known as synapses or weights and are summed together by the processing unit. Then the weighted sum is further processed by the neuron which contains an activation function that takes the weighted sum and produces an output depending upon its model. The activation function can be of any standard form depending up on the type and architecture of neural network. Based on the learning paradigms, the architecture of a neural network can be classified into two categories. There are two major paradigms of learning; supervised learning, and unsupervised learning. In supervised mode of learning, the required or desired output of neurons are known and taken as target to train the neural network for classification purposes, while, in unsupervised mode of learning the desired 'target' against an input is unknown and data is clustered into different classes based on similarity. Neural networks are techniques of machine learning algorithms and can be used as powerful tools for classification purpose, therefore, can be used for filter out the noise. In this regard, back-propagation network from supervised learning, and Self-Organizing Map (SOM) from unsupervised learning paradigm, are investigated. Moreover, K-Mean from

clustering techniques and neural network trained with Particle Swarm Optimization are also used in order to filter out background noise from different sources for a machining process.

Generally, feed forward neural network architecture consists of three layers; an input layer  $i$ , a hidden layer  $j$  and an output layer  $k$ . The learning data  $Q = \{(X_k, T_k)\}_{k=1}^E$  is drawn from the pattern space where each sample relates an input vector  $X_k \in \mathbb{R}_n$  and  $T_k \in \mathbb{R}_p$ , where  $T_k$  is a desired vector response to an input  $X_k$ . Numbers of neurons in the input layer are generally equal to number of input features while number of neurons in the output layer depend upon number of output classes. There is no fix rule to select number of neurons in the hidden layer. The number of hidden layer neurons are variable and can be chosen according to neural network performance. The feed forward network structure is shown in figure 1.

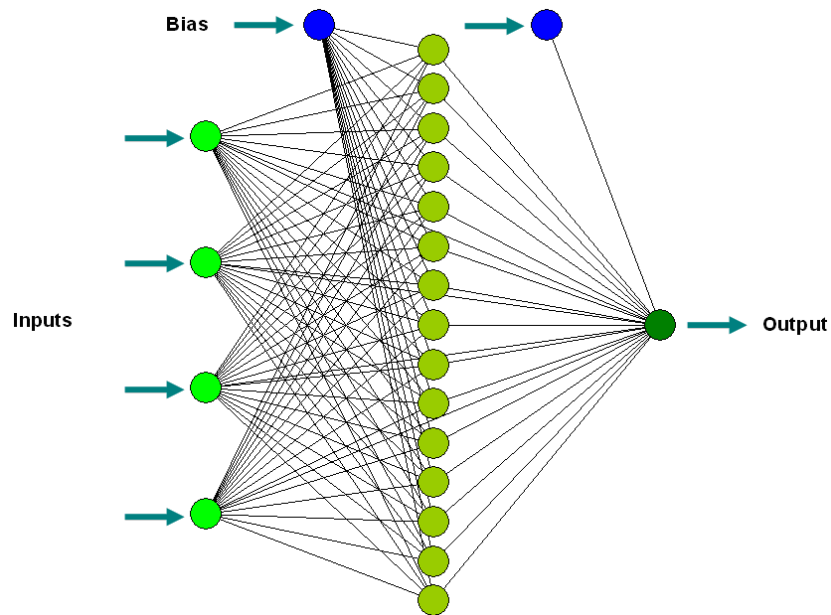


**Figure 3.1** Feed Forward Neural Network Structure [32]

The feature vector  $In = [i_1 \ i_2 \ i_3 \ \dots \ i_n]$ , is taken as input to neural network through input layer which is then amplified by gain factors or weights  $w_{ij}$  in the hidden layer. A weight vector  $b = [b_1 \ b_2 \ b_3 \ \dots \ b_n]^T$  with '1' as input is added to each neuron in the hidden layer and this weight vector is known as bias.

$$y = \sum w_{ij}i_i + b \quad (3.1)$$

Here,  $y = [y_1 \ y_2 \ y_3 \ \dots \ y_n]^T$  and

$y_i$  is the output sum against the input presented in the input layer ;  $w_{ij}$  is the weight between the hidden and input layer;  $i$  is input feature vector; and  $b$  is the bias vector.

An activation function, given by equation 3.2, is applied to sum  $y$  obtained by equation 1 to determine the hidden layer neuron output state

$$S(y) = \frac{1}{1+e^{-y}} - 1 \quad (3.2)$$

Where  $s(y)$  is output sum of input layer

The output of the activation function lies within the range of  $[0, 1]$  and is again amplified by new weights  $v_{jk}$  and is calculated using equation 1 and fed to output layer using the same procedure as mentioned above. The feed forward neural network updates its weights based on mean square error which is given by

$$MSE = \frac{1}{N} \sum_{i=1}^N (\psi(t_i; \mathbf{x}) - O_i)^2 \quad (3.3)$$

Where  $\psi(t_i; \mathbf{x})$  the output target of input feature vector, and  $O_i$  is neural network output.

The weights of neural network are updated for every input vector as provided by equation 3.4

$$W_k = W_{k-1} + \Delta W_k \quad (3.4)$$

A variety of backpropagation algorithms such as gradient descent method, gradient descent with momentum, Levenberg-Marquardt (LM) algorithm and many others are being used by researchers. We have used LM based backpropagation algorithm due to its fast convergence. The algorithm adapts the weights of neural network using the weight update rule

$$\Delta W_k = -\mu [H(W_{k-1})]^{-1} \nabla E(W_{k-1}) \quad (3.5)$$

Where  $\Delta W_k$  is change in weight;  $\mu$  is learning rate;  $\mathbf{H}$  is hessian matrix, and  $\nabla E$  is gradient of network error function.

In unsupervised learning, Self-Organizing Maps are investigated. The architecture of SOM contains only two layers; input layer, and the competitive layer as shown in figure 2. Feature vector calculated from the signals as well as recorded from the machine are taken as input, and is fed to input layer  $i$  which is then amplified by weight  $W_{ij}$ .

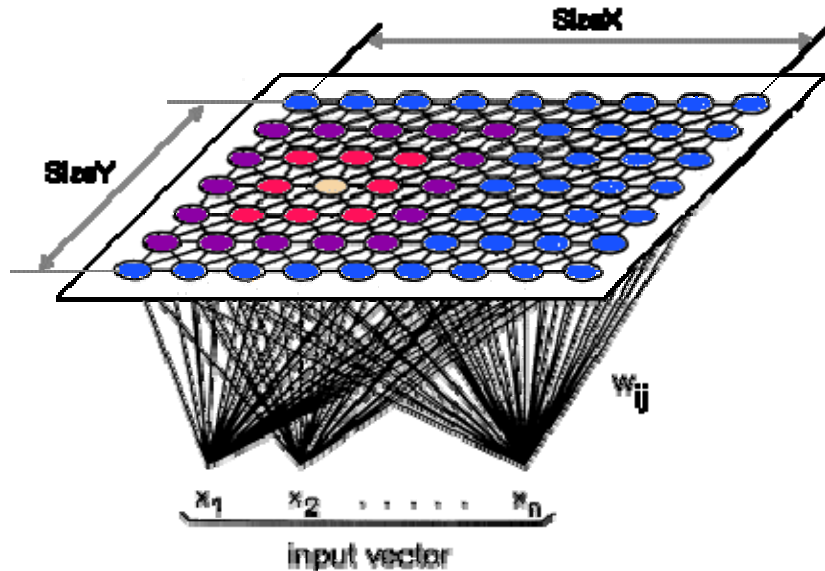


**Figure 3.2** Self-organizing map neural network structure[33]

The neural network clusters the data based on its similarity and calculates its weight based on Euclidian distance between input and neurons given by

$$\|E(j)\| = \sqrt{\sum_{i=0}^{l-1} (W_{ij} - X_i)^2} \quad (3.6)$$

Where  $E_j$  is Euclidian distance from  $j^{\text{th}}$  neuron to the input,  $W_{ij}$  is weight and  $X_{ij}$  is input vector.

The neural network then searches for a winning neuron which is a neuron with minimum distance and updates the weights of winning neuron only depending upon the conditions. Generally, a neighborhood of square, diamond or rectangle shape can be defined to update the weight of neurons in the neighbor of winning neuron.

K-Means algorithm from the clustering techniques, is investigated to assess its performance for adaptive filtering. Similar to a neural network, there are two phases of the algorithm as well; an initialization phase and a testing phase. In the training phase, the algorithm divides the data into K clusters based on distances and find the center or mean of the cluster. The initial center of clusters is chosen randomly from the data and then distance is calculated from this center using equation:

$$\|D(i, j)\| = (X_i - C_j)^2 \quad (3.7)$$

Where  $D(i, j)$  is the distance between  $i^{\text{th}}$  sample and the  $j^{\text{th}}$  center,  $X_i$  is the input sample feature, and  $C_j$  is the center of cluster

Distance between each input and cluster mean is calculated and then each input sample is assigned to a cluster with the least distance. With every iteration, mean of each cluster is updated. During the testing phase, the centers of the clusters remain stationary and each test sample is assigned to a cluster based on the distance.

In the optimization techniques, Particle Swarm Optimization (PSO) is selected to train feed forward network. PSO is an optimization technique which can be applied in order to optimize the weights of already trained neural network. The optimization of the weights has been done for tool health monitoring application. Please refer to our paper [34]. Here, PSO was used to optimize the neural network weights trained with gradient-descent method. However, when the neural network is trained with Levenberg-Marquardt algorithm, the results were better. Hence, performance of PSO is investigated to train the neural network rather than optimizing an already trained neural network.

PSO is a bio-inspired optimization algorithm that takes its inspiration from the flocking pattern of the birds which they form for the food search. It starts with the initialization of a group of random particles that may represent a possible solution to a problem against a fitness function. It then searches for an optimal value by updating the particles position and velocity for each generation using two best values. Particle best  $P_i$ , the best solution a particle can have so far and the Global best  $P_g$ , which is maintained by the PSO algorithm as the best value obtained so far by

any particle in the population. The velocity and position of a particle is given by equation 3.7 and 3.8 respectively.

$$V_j(t) = \omega(t)V_j(t-1) + C_1R_1(P_i(t-1) - X_j(t-1)) + C_2R_2(P_g(t-1) - X_j(t-1)) \quad (3.8)$$

$$X_j(t) = V_j(t) + X_j(t-1) \quad (3.9)$$

Where,  $\omega$  is inertia weight,  $V_j$  is particle velocity;  $C_1$ ,  $C_2$  are learning weights;  $R_1$  and  $R_2$  are two random numbers in the range between 0 and 1;  $P_i(t-1)$  is the best position so far while  $P_g(t-1)$  is the global best value;  $X_j$  is the particle position. A larger value of inertia weight may lead to global exploration while its smaller values may lead to local exploration of possible optimum solution[35]. Value of inertia weight is given by equation 3.10:

$$\omega(k) = \omega_{max} - \frac{I}{I_{max}}(\omega_{max} - \omega_{min}) \quad (3.10)$$

where  $\omega_{max}$  and  $\omega_{min}$  are maximum and minimum inertia weights, and  $I$  is the iteration number.

Pseudo algorithm of PSO is given as:

**Step 1:** For every particle  $j$ ,

Initialize  $X_j(t)$  and  $V_j(t)$

End

For every particle  $j$ , do steps 2 to 5

**Step 2:** Compute MSE $\beta$

**Step 3:** If  $\beta > X_j(t-1)$ , Set current value as new pbest

**Step 4:** select the particle with best fitness value as the gbest

**Step 5:** calculate  $X_j(t)$  value using equation

**Step 6:** Update and  $V_j(t)$  using equation

*End*

## 3.2. Signal reconstruction

To reconstruct the filtered signal, a novel Auto Regressive Moving Average (ARMA) based reconstruction algorithm is developed. ARMA is a time series model that has been used in other fields of research in order to predict the forecast of different systems such as sunspot data, rain prediction system, prediction of dam inflow of dam reservoir etc., however, it has not been used to reconstruct the signal.

ARMA is combination of Auto Regressive Model of order (p)

$$x_{t+1} = x_t + \varphi_1 x_{t-1} + \dots + \varphi_p x_{t-p} + \delta \quad (3.10)$$

and Moving Average Model of order (q)

$$x_{t+1} = \varepsilon_t + \theta_1 \varepsilon_{t-1} + \dots + \theta_q \varepsilon_{t-q} \quad (3.11)$$

where  $\varphi_i, \theta_i$  are the model coefficients,  $x_t$  is the previous sample value and  $\varepsilon_t$  is the white noise error. In general, autoregressive model determines that the current value of the system depends on how many previous terms? Whereas, the MA models are “averages” of the past and present noise terms

AR and MA model can be combined to form ARMA which can be mathematically defined as:

$$x_t = x_t + \varphi_1 x_{t-1} + \dots + \varphi_p x_{t-p} + \varepsilon_t + \theta_1 \varepsilon_{t-1} + \dots + \theta_q \varepsilon_{t-q} \quad (3.12)$$

In order to estimate ARMA model, Box and Jenkins method[36] is used here. There are two basic steps of the ARMA model estimation.

- Identification of ARMA order
- Estimation of ARMA coefficients

### 3.2.1. Identification of model order:

One of the pre-requisite condition of the time series model is that the series must be stationary[37]. A series is said to be stationary if the joint probability distribution of any  $n$  observations  $\{x_{t+1}, x_{t+2}, x_{t+3}, \dots, x_{t+n}\}$  of the series remains the same as another set of  $n$  observations shifted by  $k$  units i.e.  $\{x_{t+1+k}, x_{t+2+k}, x_{t+3+k}, \dots, x_{t+n+k}\}$ . To make the series stationary,  $M^{\text{th}}$  order difference can be taken. Generally value of  $M$  is set to be 1 or 2, however, care must be taken in selecting the value of  $M$  to avoid under or over differencing of the series. An under differenced series may behave as non-stationary series while an over differenced series may behave as stationary series, however, the estimation of coefficients would be difficult in this case.

Two separate tests are used to determine the order of AR model and MA model. These test are Autocorrelation Function test and Partial Autocorrelation Function test. Autocorrelation function test shows how correlated the observations are, that are  $k$  lags apart, and is used to identify the order of MA model. Mathematically, ACF can be defined as

$$C_x(h) = \frac{1}{T} \sum_{t=1}^{T-h} (x_t - \bar{x})(x_{t+h} - \bar{x}) \quad (3.13)$$

$$r_h = \frac{C_x(h)}{C_x(0)} \quad (3.14)$$

Number of peaks outside the upper and lower bounds determine the order of MA model. Figure 3.3 showing a sample autocorrelation function according to which order of MA model should be 2 since two peaks can be seen at lag 1 and lag 2.

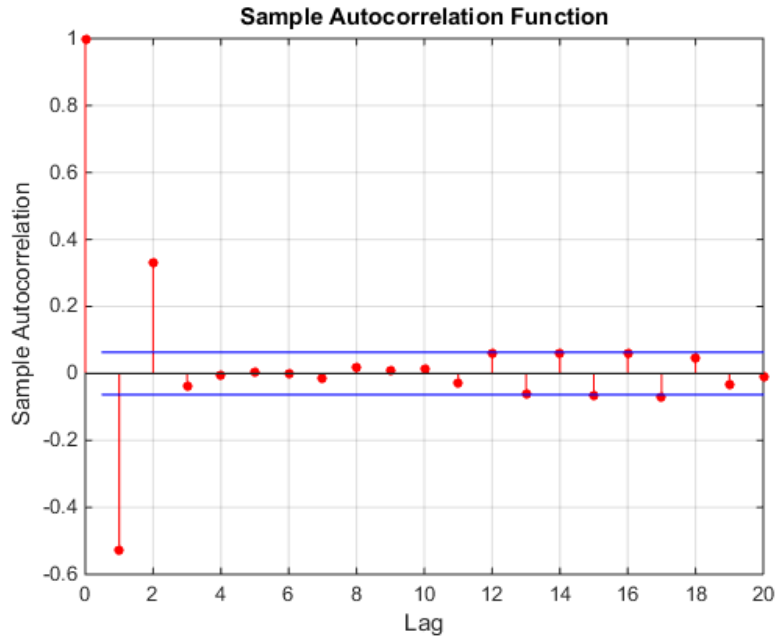


**Figure 3.3** Autocorrelation function[38]

The partial autocorrelation function can be interpreted as a regression of the series against its past lags and is used to determine the order of AR model. Mathematically, PACF can be calculated as

$$\chi_{kk} = \frac{\begin{vmatrix} 1 & r_1 & \dots & r_1 \\ r_1 & 1 & \dots & r_2 \\ \vdots & \vdots & \ddots & \vdots \\ r_{k-1} & r_{k-2} & \dots & r_k \end{vmatrix}}{\begin{vmatrix} 1 & r_1 & \dots & r_{k-1} \\ r_1 & 1 & \dots & r_{k-2} \\ \vdots & \vdots & \ddots & \vdots \\ r_{k-1} & r_{k-2} & \dots & 1 \end{vmatrix}} \quad (3.15)$$

Similarly, PACF provides an indication of order of AR model. AR model will be of Mth order if M peaks are outside the 95% confidence level. In figure 3.4, value of M is 2.

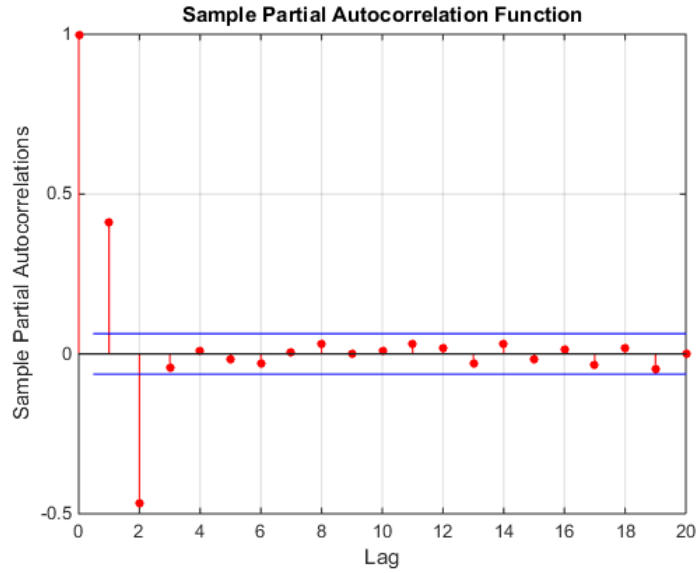


**Figure 3.4** Partial Autocorrelation function[39]

There are two tests to check the proper order of the difference for the series; ACF test and, variance test. ACF plot can be used to test the under differencing of the series. If ACF of the series dies out quickly, then it means that the series is stationary, otherwise the series is non-stationary and series must be differenced. Figure 3.3 shows the ACF example of stationary and non-stationary series.

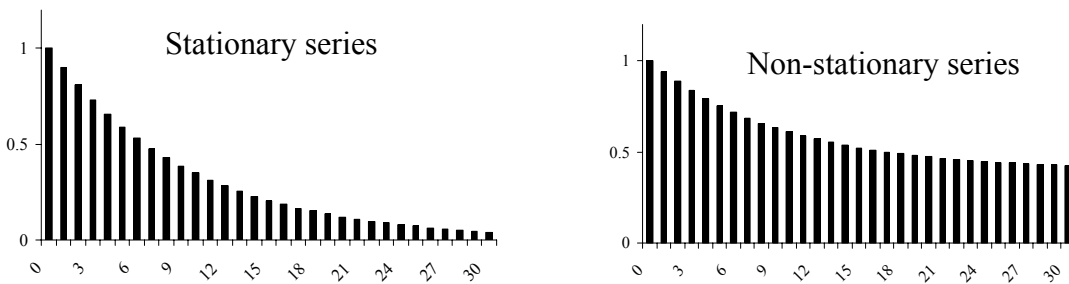


**Figure 3.5** ACF test for stationary and non-stationary series[37]

In order to determine the over differencing of the series, variance test can be used. According to variance test, variance of a stationary series is minimum. It means that variance of the different

order differenced series can be recorded and the minimum value of variance will determine the proper order of difference that is needed to be taken to make the series stationary.

### 3.2.2. Estimation of model coefficients

The second step of ARMA model estimation is to determine the value of its coefficients. This is done by Maximum Likelihood Method. Maximum Likelihood Estimation selects the values as estimators of a set of parameters that maximize

$L(q_1, q_2, q_3, \dots, q_k) = f(x_1, x_2, x_3, \dots, x_N; q_1, q_2, q_3, \dots, q_k)$  where  $f(x_1, x_2, x_3, \dots, x_N; q_1, q_2, q_3, \dots, q_k)$  is the joint density function of the observations  $x_1, x_2, x_3, \dots, x_N$ .  $L(q_1, q_2, q_3, \dots, q_k)$  is called the **Likelihood function**. Finding the values  $q_1, q_2, q_3, \dots, q_k$  to maximize  $L(q_1, q_2, q_3, \dots, q_k)$  is equivalent to finding the values to maximize  $l(q_1, q_2, q_3, \dots, q_k) = \ln(L(q_1, q_2, q_3, \dots, q_k))$  which is called the **log-Likelihood function**[37].

Consider the time series defined by equation 3. 12. To estimate the  $p + q + 2$  parameters  $\varphi_1, \varphi_2, \varphi_3, \dots, \varphi_p; \theta_1, \theta_2, \theta_3, \dots, \theta_q; \delta; \sigma^2$  by the method of Maximum Likelihood Estimation we need to find the joint density function of the observations  $x_1, x_2, x_3, \dots, x_N$  i.e.,  $f(\varphi_1, \varphi_2, \varphi_3, \dots, \varphi_p; \theta_1, \theta_2, \theta_3, \dots, \theta_q; \delta; \sigma^2) = f(\mathbf{x}|\boldsymbol{\varphi}, \boldsymbol{\theta}, \delta, \sigma^2)$

It is difficult to determine the exact density function of  $x_1, x_2, x_3, \dots, x_N$  from this information however if we assume that  $p$  starting values on the AR model  $\mathbf{x}^* = x_{1-p}, x_{2-p}, x_{3-p}, \dots, x_0$  and  $q$  starting values on the MA model  $\mathbf{u}^* = u_{1-p}, u_{2-p}, u_{3-p}, \dots, u_0$  have been observed then the conditional distribution of given  $x_1, x_2, x_3, \dots, x_N$   $\mathbf{x}^* = x_{1-p}, x_{2-p}, x_{3-p}, \dots, x_0$ , and  $\mathbf{u}^* = u_{1-p}, u_{2-p}, u_{3-p}, \dots, u_0$  can easily be determined. The joint density of  $\mathbf{x}$  given  $\mathbf{x}^*$  and  $\mathbf{u}^*$  can be calculated by conditional likelihood function is given by:

$$L_{\mathbf{x}|\mathbf{x}^*, \mathbf{u}^*}(\boldsymbol{\varphi}, \boldsymbol{\theta}, \delta, \sigma^2) = \left(\frac{1}{\sqrt{2\pi\sigma}}\right)^n \exp\left\{-\frac{1}{2\sigma^2} \sum_{t=1}^N u_t^2(\mathbf{x}^*, \mathbf{u}^*, \boldsymbol{\varphi}, \boldsymbol{\theta}, \delta)\right\}$$

$$= \left(\frac{1}{\sqrt{2\pi\sigma}}\right)^n \exp\left\{-\frac{1}{2\sigma^2} \kappa^*(\boldsymbol{\theta}, \boldsymbol{\varphi}, \delta)\right\} \quad (3.16)$$

where

$$\kappa^*(\boldsymbol{\theta}, \boldsymbol{\varphi}, \delta) = \sum_{t=1}^N u_t^2(\mathbf{x}^*, \mathbf{u}^*, \boldsymbol{\varphi}, \boldsymbol{\theta}, \delta)$$

Conditional log likelihood function can be calculated by taking ln on both sides

$$l_{x|x^*, u^*}(\boldsymbol{\varphi}, \boldsymbol{\theta}, \delta, \sigma^2) = \ln(L_{x|x^*, u^*}(\boldsymbol{\varphi}, \boldsymbol{\theta}, \delta, \sigma^2)) \quad (3.17)$$

$$= -\frac{n}{2} - \frac{n}{2} \ln(\sigma^2) - \frac{1}{2\sigma^2} \sum_{t=1}^N u_t^2(\mathbf{x}^*, \mathbf{u}^*, \boldsymbol{\varphi}, \boldsymbol{\theta}, \delta)$$

$$= -\frac{n}{2} - \frac{n}{2} \ln(\sigma^2) - \frac{1}{2\sigma^2} \kappa^*(\boldsymbol{\theta}, \boldsymbol{\varphi}, \delta) \quad (3.18)$$

The values that maximize  $l_{x|x^*, u^*}(\boldsymbol{\varphi}, \boldsymbol{\theta}, \delta, \sigma^2)$  and  $L_{x|x^*, u^*}(\boldsymbol{\varphi}, \boldsymbol{\theta}, \delta, \sigma^2)$  are the values  $\hat{\boldsymbol{\varphi}}, \hat{\boldsymbol{\theta}}, \hat{\delta}$  that minimize  $\kappa^*(\boldsymbol{\theta}, \boldsymbol{\varphi}, \delta) = \sum_{t=1}^N u_t^2(\mathbf{x}^*, \mathbf{u}^*, \boldsymbol{\varphi}, \boldsymbol{\theta}, \delta)$  with  $\hat{\sigma}^2 = \frac{1}{n} \sum_{t=1}^N u_t^2(\mathbf{x}^*, \mathbf{u}^*, \hat{\boldsymbol{\varphi}}, \hat{\boldsymbol{\theta}}, \hat{\delta}) = \frac{1}{n} \kappa^*(\hat{\boldsymbol{\theta}}, \hat{\boldsymbol{\varphi}}, \hat{\delta})$

### 3.2.3. Proposed algorithm for signal reconstruction

An ARMA based algorithm is developed to reconstruct the filtered signal. In order to determine the order of the ARMA model, at least 50 samples from the signals are needed. For first 50 samples, the sample values of the machining signal that are filtered falsely by the algorithm are replaced by the values determined by average of the two neighboring samples. After replacing the falsely filtered values, ARMA model is estimated using the first 50 samples. Then the developed algorithm, move the sampling window to next 50 samples and forecast N sample points if there is any filtered values, in order to reconstruct the signal. The developed algorithm can forecast up to 5 sample points without moving window further. In order to reconstruct more than 5 sample points, the algorithm first forecast 5 samples and then move the window to next 50 samples and then check for number of filtered samples. The process continues until the whole signal is reconstructed. After the complete signal is reconstructed, the reconstruction algorithm takes the

average of the forecasted or reconstructed samples, and update the false negatives values of the first 50 samples.

Summary of the proposed algorithm is shown in figure 3.1

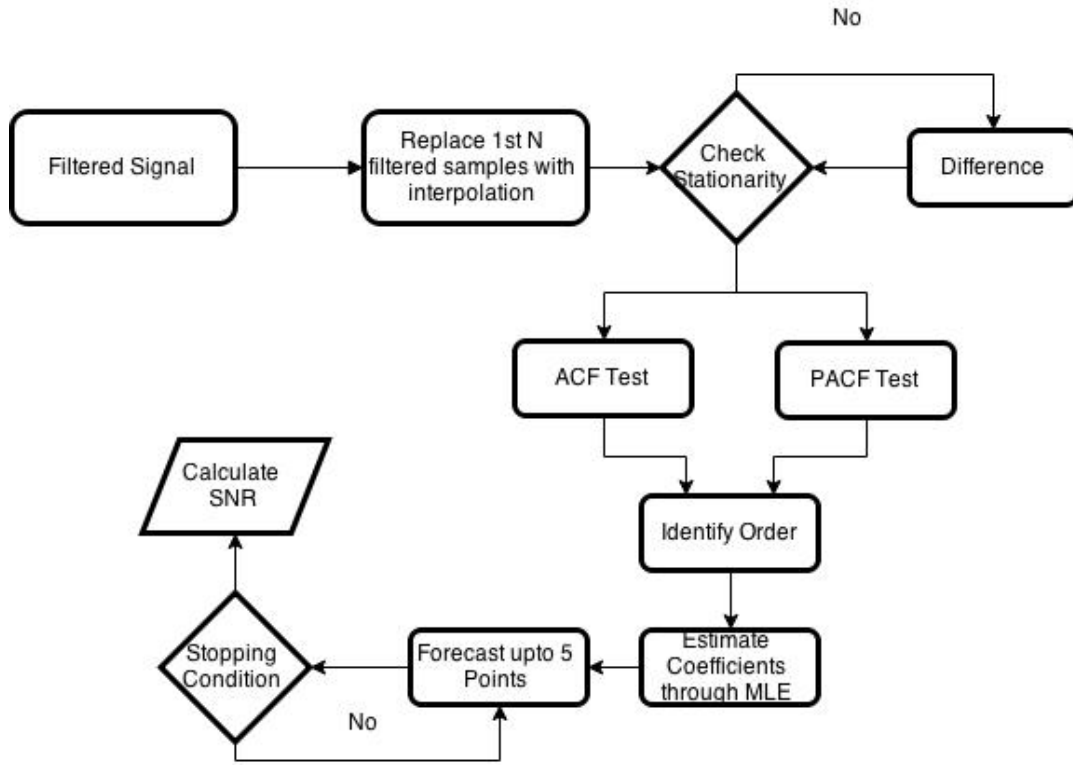


**Figure 3.6** ARMA based reconstruction algorithm flowchart

Summary of the proposed algorithm is shown in figure 3.4.

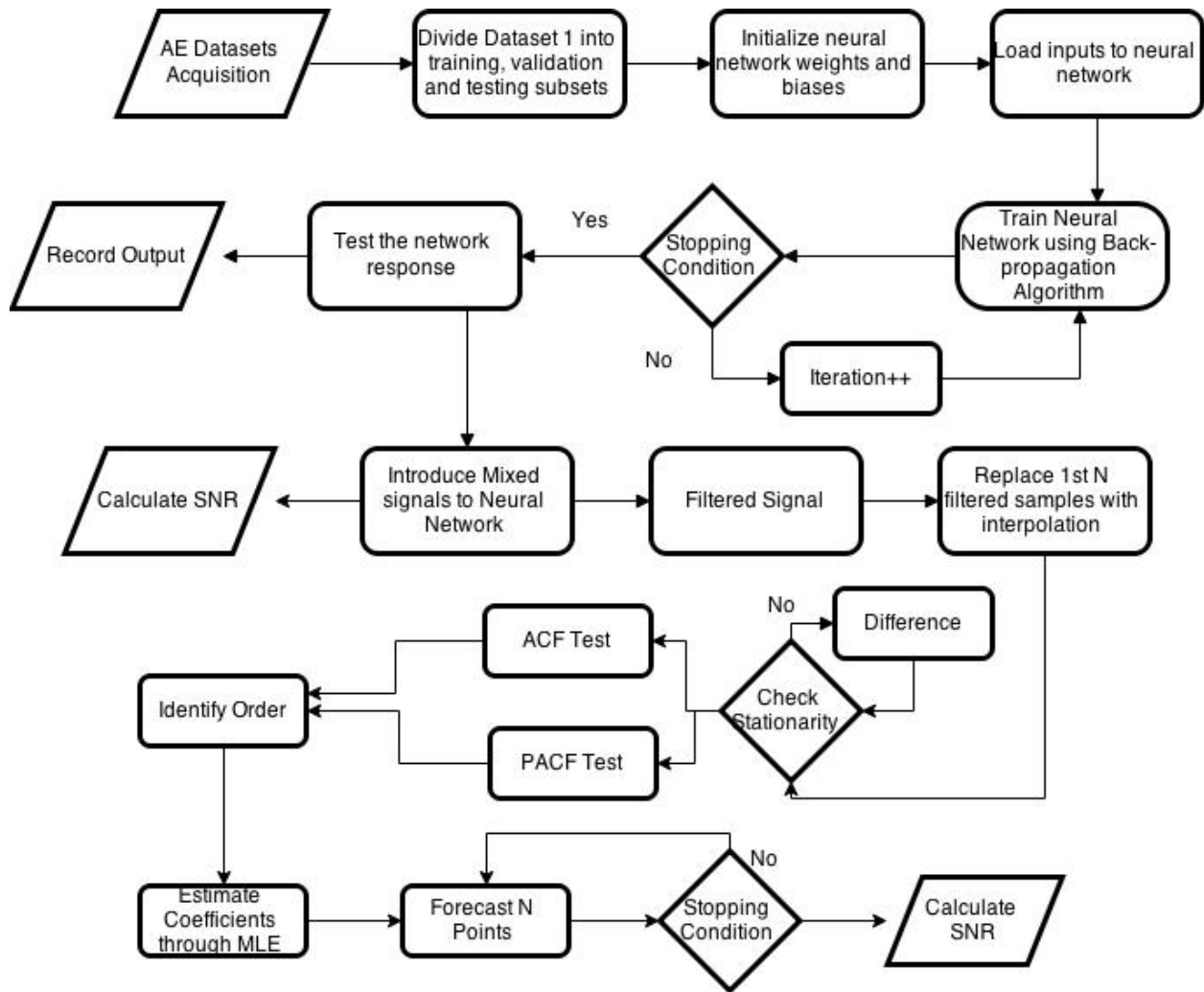


**Figure 3.7** Flowchart of proposed algorithm

### 3.3. Summary

The chapter can be summarized as follows:

- ❖ Machine Learning algorithms can be used as adaptive filters in the time domain. Traditional filters cannot be employed in the case when frequencies of noise are variable and can lie within the range of machining signal.
  
- ❖ Different paradigms of machine learning algorithms are selected in order to compare their performance. These techniques include, backpropagation neural network, Self-Organizing Maps, K-Means algorithm and a feed-forward neural network trained with Particle Swarm Optimization.
  
- ❖ Signal reconstruction can be done using a statistical time series model. A novel ARMA based algorithm is proposed which has never been used for a machining process in the literature so far.

## 4. EXPERIMENTATION

This chapter provides details about the experimental setup and signal acquisition. A table of various features of acquired signal is also presented. Details about parallel running machines signals are also shown and discussed here.

### 4.1. Experimental setup

Experiments are conducted in Industrial Automation Lab of college of EME, National University of Sciences and Technology, Islamabad, Pakistan. Acoustic signals for a turning process are acquired from a Denford Cyclone P CNC machine tool. The signals are acquired using a microphone at a rate sampling rate of 44100 Hz in order to fulfill the Nyquist criteria. Each signal is recorded for a duration of 10 seconds. Figure 4.1 shows the experimental setup while figure 4.2 shows the close view of the microphone setup.



**Figure 4.1** Experimental setup

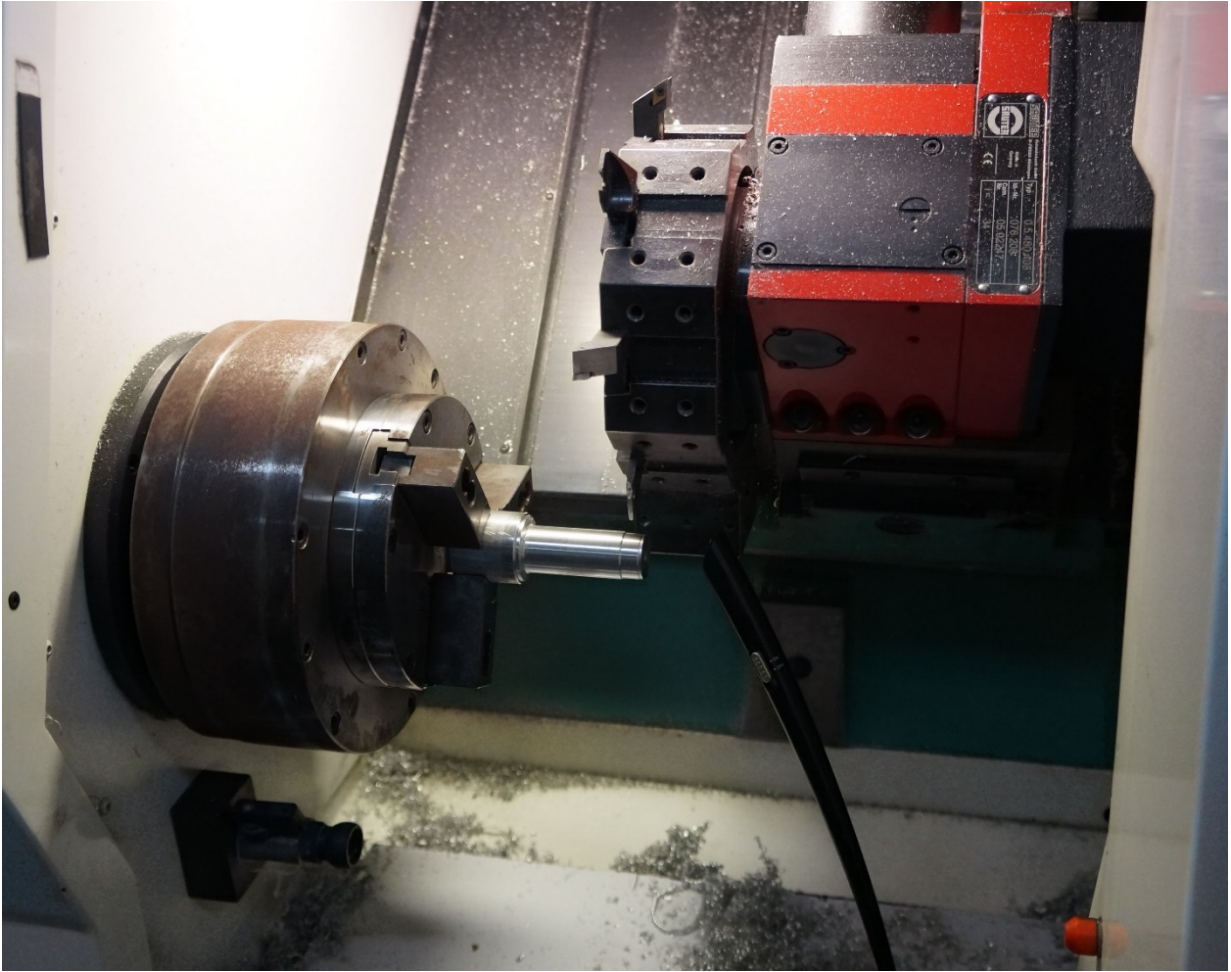


**Figure 4.2** Close view of microphone setup

A total of 27 machining signals are recorded at different RPMs and feed rates, at constant depth of cut. Some of the calculated statistical features of the acquired data are tabulated in table 1. Skewness and kurtosis of the recorded data are presented in the table in addition to basic statistical features, such as mean and standard deviation. Skewness of a signal is defined as the third moment about the mean[40]. It determines the symmetry of a signal about the mean. Similarly, kurtosis of a signal can be defined as fourth moment about the mean and it determines the sharpness of the peak of the signal.

**Table 4-1** Various features of acquired signals

Test No.	Sample No.	Speed (RPM)	Feed Rate (mm/s)	Mean	Standard Deviation	Kurtosis	Skewness	Max	Min	RMS max
1	1	1016	200	-1.7465e-05	0.0044	2.9318	0.0136	0.0191	-0.0152	0.1137
2	2	1016	200	-1.8136e-05	0.0046	2.9340	0.0195	0.0192	-0.0161	0.0063
3	3	1016	200	-1.7098e-05	0.0045	2.9543	0.0038	0.0194	-0.0151	0.0058
4	1	1016	400	-1.5636e-05	0.0052	3.1213	0.0011	0.0235	-0.0196	0.0091
5	2	1016	400	-1.6354e-05	0.0049	3.1899	-0.0258	0.0561	-0.0212	0.0071
6	3	1016	400	-1.5471e-05	0.0054	3.1457	0.0251	0.0274	-0.0213	0.0095
7	1	1016	600	-1.6338e-05	0.0055	3.3991	0.0611	0.0298	-0.0253	0.0108
8	2	1016	600	-1.8543e-05	0.0046	3.0040	0.0439	0.0202	-0.0161	0.0062
9	3	1016	600	-1.4868e-05	0.0068	4.3357	-0.0548	0.0460	-0.0444	0.0201
10	1	1522	200	-1.7455e-05	0.0055	2.9679	0.0087	0.0222	-0.0219	0.0079
11	2	1522	200	-1.6204e-05	0.0056	3.0014	0.0120	0.0255	-0.0194	0.0075
12	3	1522	200	-1.5330e-05	0.0060	3.1795	-0.0256	0.0277	-0.0269	0.0107
13	1	1522	400	-1.2834e-05	0.0061	3.2998	-0.0347	0.0407	-0.0273	0.0119
14	2	1522	400	-1.4114e-05	0.0055	4.0949	0.0081	0.0865	-0.0212	0.0109
15	3	1522	400	-1.6224e-05	0.0054	2.9845	0.0071	0.0233	-0.0182	0.0075
16	1	1522	600	-1.9518e-05	0.0062	3.9978	-0.0397	0.0396	-0.0424	0.0158
17	2	1522	600	-1.8584e-05	0.0056	3.0727	0.0117	0.0256	-0.0213	0.0088
18	3	1522	600	-1.6196e-05	0.0057	3.0663	0.0153	0.0347	-0.0233	0.0092
19	1	2000	200	-1.5051e-05	0.0057	2.9056	0.0158	0.0250	-0.0200	0.0083
20	2	2000	200	-1.6886e-05	0.0059	2.9688	-0.0105	0.0279	-0.0227	0.0091
21	3	2000	200	-1.5876e-05	0.0059	3.0455	0.0503	0.0292	-0.0283	0.0096
22	1	2000	400	-1.3383e-05	0.0055	2.9997	0.0364	0.0249	-0.0195	0.0083
23	2	2000	400	-1.7215e-05	0.0055	3.0126	0.0463	0.0244	-0.0199	0.0079
24	3	2000	400	-1.5613e-05	0.0057	3.0517	0.0340	0.0249	-0.0209	0.0078
25	1	2000	600	-1.6459e-05	0.0061	2.9768	0.0330	0.0287	-0.0223	0.0101
26	2	2000	600	-1.4762e-05	0.0063	2.9606	0.0501	0.0269	-0.0234	0.0089
27	3	2000	600	-1.5195e-05	0.0063	3.2031	0.0403	0.0318	-0.0289	0.0121

If  $i^{\text{th}}$  central moment of signal  $\zeta_i$  is defined as:

$$\zeta_i = E[(s - \bar{s})^i] \quad (4.1)$$

Where  $J$  is the moment,  $s$  is machining signal in time domain, then the normalized third moment can be defined as:

$$S_k = \frac{\zeta_3}{\sigma^3} \quad (4.2)$$

Where  $\zeta$  is the moment and  $\sigma$  is the standard deviation.

Similarly, as explained above, kurtosis is the fourth moment about the mean is given by:

$$K_x = \frac{\zeta_4}{\sigma^4} \quad (4.3)$$

Where  $\zeta$  is the moment and  $\sigma$  is the standard deviation

RMS of a signal is considered as a dominant feature of a machining signal as it varies with the increase in degradation of tool health. Many researchers has considered it to be the most significant feature for tool health monitoring[41, 42, 43, 44]. RMS of a signal can be calculated for a specific window length as:

$$S_{rms} = \sqrt{\frac{s_1^2 + s_2^2 + \dots + s_n^2}{n}} \quad (4.4)$$

Where  $s_i$  is data sample and  $n$  is total number of sample points in a window.

A raw acoustic signal recorded at a feed rate of 200 mm/sec and a constant depth of cut of 0.5 mm for a turning process is shown in figure 4.3(a). The RMS of the signal is then calculated in the time domain for a window length of 1000 samples. Figure 4.3(b) shows the RMS plot of the same signal.

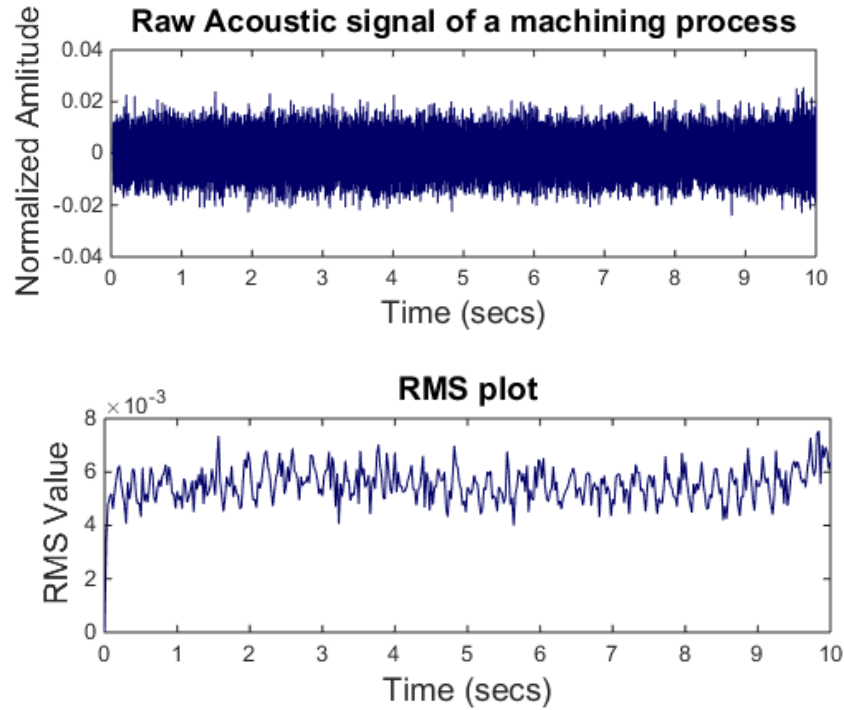


**Figure 4.3**(a) Raw acoustic signal (above), (b) RMS level of the signal

In order to validate the acquired signal from the microphone, FFT of the machining signal is calculated. This is shown in figure 4.4. As the signal was acquired at 1522 RPM, therefore, a clear peak at 25.4 Hz can be seen in the figure.

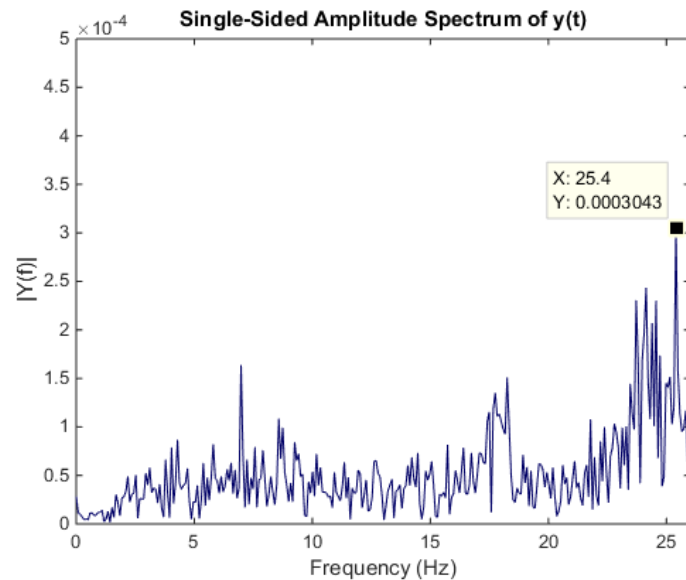


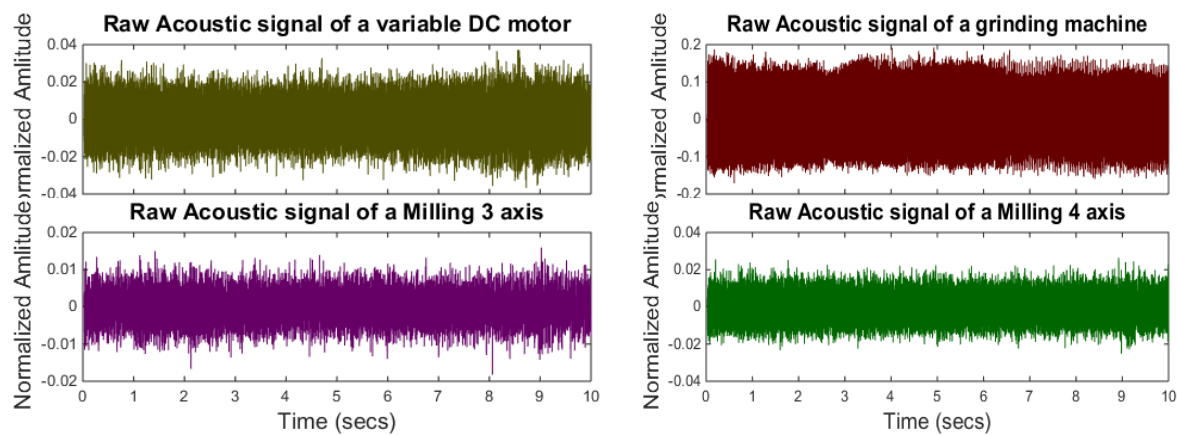
**Figure 4.4** FFT plot of machining signal

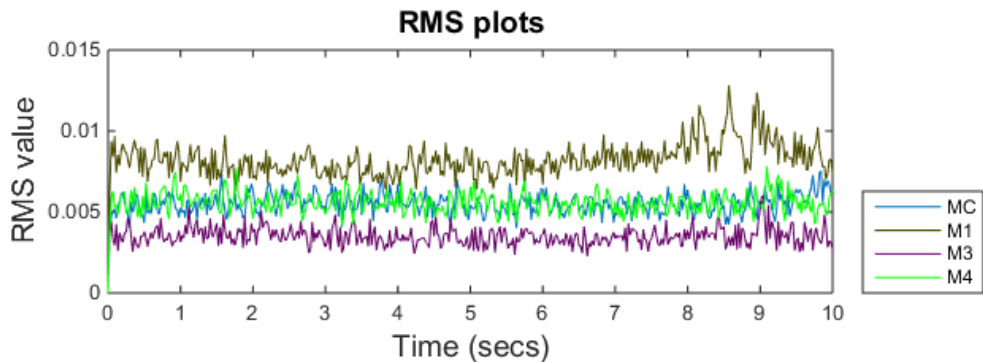
As mentioned in the chapter 2, the machining signal can be affected by various types of environmental noise, for example, if an operator sneezes, or a telephone rings in the background etc. However, for the research, only parallel running machine noise is considered. Normally, on a shop floor, where different machines are working at the same time, signals from other machines are a major source of noise. Therefore, in addition to the machining signal, signals from different machines working in the background are also recorded. These signals are considered as background noise. In this regard, four machines, a variable speed DC motor, a grinding machine, a 3-axis CNC milling machine and a 4-axis mini milling machine are selected and their signals are recorded. These machines are denoted as M1, M2, M3 and M4 while the CNC machine is denoted as MC. The distance between the CNC machine and the background machines are fixed, however, each machine has specific distance from the CNC machine. The distance between CNC machine and background machines are given in table 4.2.

**Table 4-2** Background machine distance measures

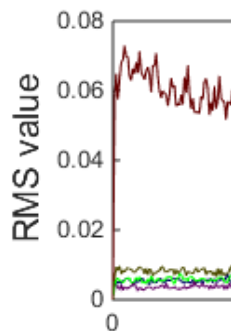
Machine	Approx. Distance
A variable speed DC motor	6m
Grinding Machine	3m
3-axis Milling Machine	1m
4-axis Mini-milling machine	3m

Figure 4.5 shows acoustic signals of the selected background machines while figure 4.6 shows the RMS level of the signals.





**Figure 4.5** Raw acoustic signals of background noise



**Figure 4.6(a)** RMS plot of machines (above),(b) RMS plot of grinding machine (below)

It can be seen from the figure 4.6 (a) that machine 4 signal has overlapping RMS level with MC i.e., machining signal RMS. As it is clear from the figure 4.6 (b) that the grinding machine signal was quite dominant and its RMS level is much higher than the rest of the machines signals.

Two datasets, dataset A and dataset B are recorded for each type of signal. For dataset A, machining signal having a length of 1 sec and signals from each background machine having length of 0.25 sec are recorded. RMS of the signals is calculated using a non-overlapping window length of 1000 samples and taken as input feature. In other words, dataset A consists of total 881 RMS samples in which 441 samples are from machining signal while 440 samples are from background machines signal; 110 samples from each machine. This data is used for the training purposes only.

For dataset B, signals, having length of 1 sec, from machining as well as background machines are recorded. Similarly as above, RMS level of the signals are calculated and taken as important feature. Hence, dataset B consists of 2205 RMS samples with 441 samples from each machine. This dataset is used only to test the machine learning algorithms.

## **4.2. Summary**

The chapter can be summarized as follows

- ❖ Acoustic signals for a turning process are acquired at different RPM, feedrate and a constant depth of cut of 0.5mm. Among the various features of the signals, RMS level is selected as a significant feature because of its linear relationship with tool degradation.
- ❖ Various types of noise can affect the machining signal, however, only parallel running machine noise are considered for the research. Four machines are selected in this regard.
- ❖ Machine 2 sound was quite dominant, therefore, it has much higher RMS level than other signals, whereas, machine 4 has RMS level which is almost equal to machining signal RMS.

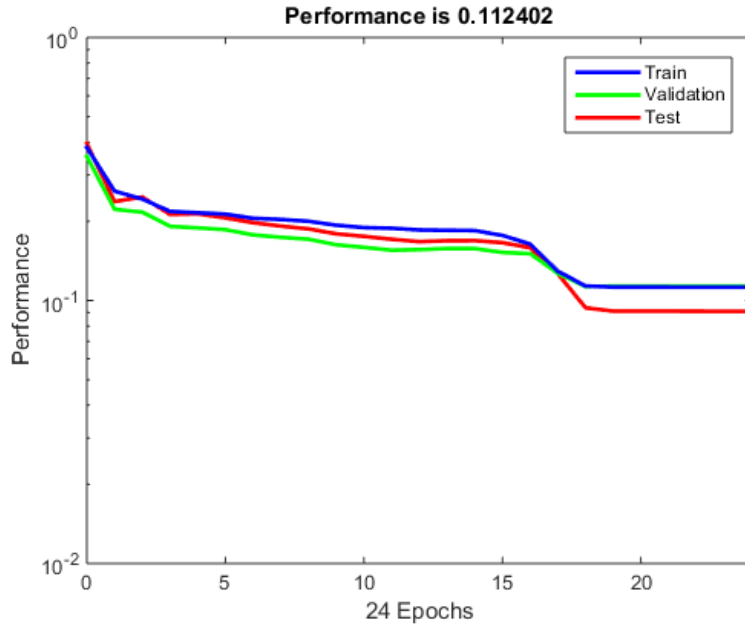
## **5. RESULTS AND DISCUSSION**

This chapter presents the results of the research. A detailed discussion on performance of different machine learning algorithms used as adaptive filters is given in the chapter. Results of signal reconstruction using ARMA are also included in the chapter.

## 5.1. Adaptive filtering

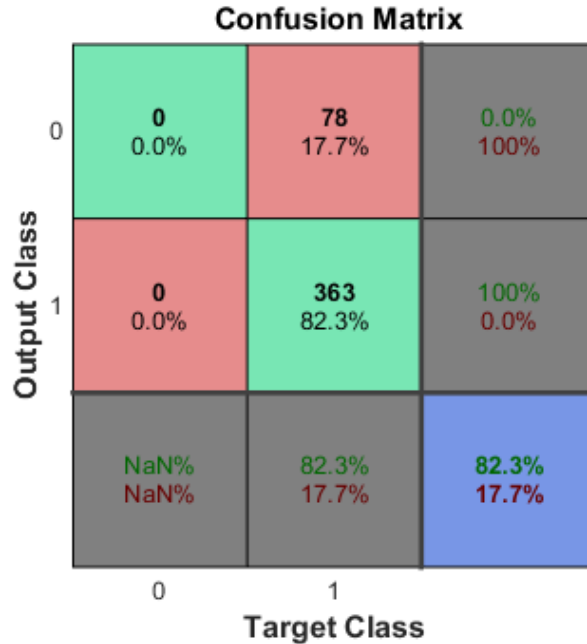
Adaptive filters are the system which adapt itself according to given environmental conditions. As mentioned earlier, different machine learning algorithms are selected in order to filter out the background noise reduction. These algorithms include back-propagation neural networks, self-organizing maps, Kmean clustering and Particle Swarm Optimization. Four distinct features, RMS, RPM, feed rate, and depth of cut are used as input to these algorithms. Two separate datasets, dataset A and dataset B are recorded and used for training and testing purposes. Dataset A is used to train the algorithms while the dataset B is used for testing purposes only.

Figure 5.1 shows the training curve for a three layer feed-forward back-propagation neural networks. The architecture of neural network consists of 4, 10 and 1 neurons in the input, hidden layer, and output layer respectively. Dataset A consists of 881 RMS samples is used for training the neural network. The dataset is further divided into three sub-datasets with 70% samples used for training purpose, 15% used for validation purpose and remaining data used for testing. Neural network is trained until the minimum value of validation error is found, which is 0.1124 as shown in figure. Training curve of back-propagation neural network is presented in figure 5.1.



**Figure 5.1** Training curve of back-propagation neural network

The performance of neural network is tested with dataset B, which contains all signals from CNC machine as well as the background machines. For machining signal, the neural network showed an accuracy of 82.3%, whereas, for M1 it is found to be 96.1%. Accuracy in case of M2 is found to be maximum i.e., 100% for grinding machine. This is because of the reason that the acoustic signal of M2 is clearly distinguishable and dominant. Accuracy in case of M3 is found to be 95.7%. The neural network showed worst performance for M4 and shows an accuracy of only 5%. One of the possible reason of the low accuracy of M4 is that RMS level of M4 is overlapping with machining signal RMS as shown in figure 4.6 (a). Figure 5.2 shows the confusion matrix of the back-propagation neural network for machining signal; class 1 is targeted for machining signal, whereas, class 0 represents the background noise or signals from other sources.



**Figure 5.2** Confusion matrix for machining signal

Training response for SOM network is shown in figure 5.3. Here again, 881 sample points from dataset A are used to train the network, out of which 441 belongs the machining signal, whereas, 440 sample points, out of which, 110 each represent background noise from each source. The network is trained for 300 epochs.

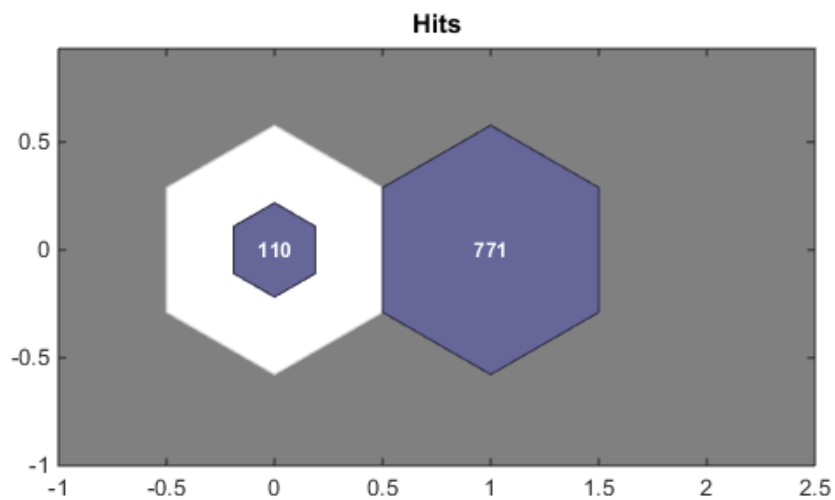


**Figure 5.3** Self-Organizing Map Neural Network clusters for training data

As shown in the above figure, the data is classified into two clusters; cluster one for the machining signal, and cluster two for background signals that are taken as noise, however, not all of them are truly classified. It is clear from figure 5.3 that 110 samples are classified as background noise, while 771 sample points are clustered as machining signal. This is because of the reason that the sample points of the background noise that are closer to the machining signal are classified wrongly by the SOM networks as machining data. This is the initial phase of cluster formation. However, to assess the performance, SOM is tested for each type of signal from dataset B. SOM network is found to be 100% for machining signal as well as 99.7% accurate for grinding machine (M2). However, SOM showed worst accuracy for M1, M3, and M4. Figure 5.4 shows the network response for machining signal.

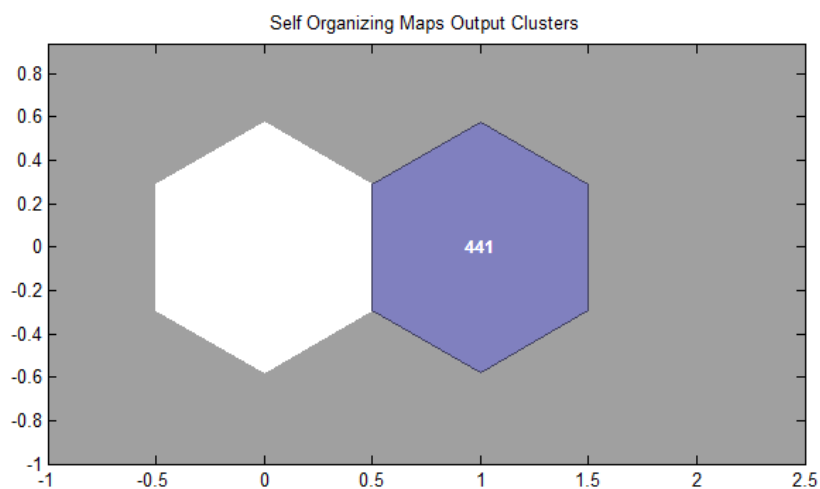


**Figure 5.4** SOM response for machining signal

Initial cluster formation using K-means algorithm for machining signal as well as background noise is shown in figure 5.5. In the figure, sample numbers are taken on x-axis, while, RMS value of the signal is shown on y-axis. The data means or two centroids are represented by a bold 'X'. As it is clear from the figure, two clusters are formed; one cluster for the machining signal and the other for the background noise from different sources.

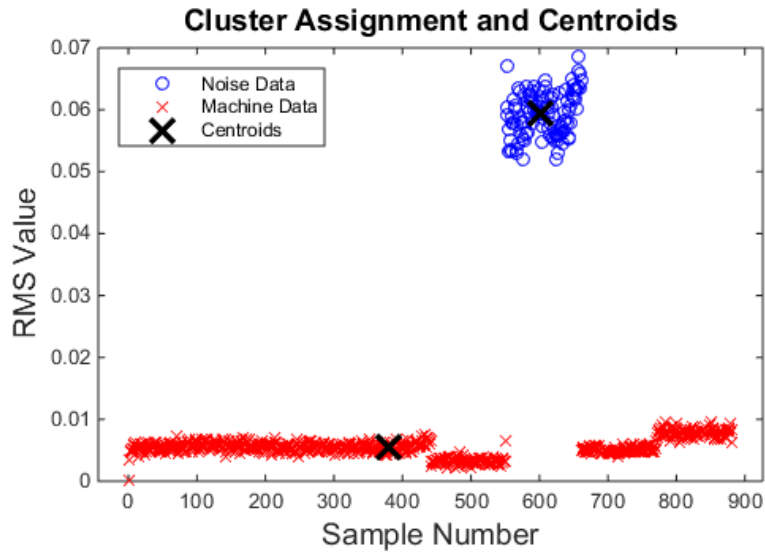


**Figure 5.5**K-Means training data clustering

Dataset A is used to calculate the cluster mean. Out of 881 samples from the dataset A, 771 are classified as machining signal and 110 are classified as background noise. However, out of 771 samples that are classified as machining signal 330 are false positives. Figure 5.6 shows the response of k-means algorithm for machining signal.

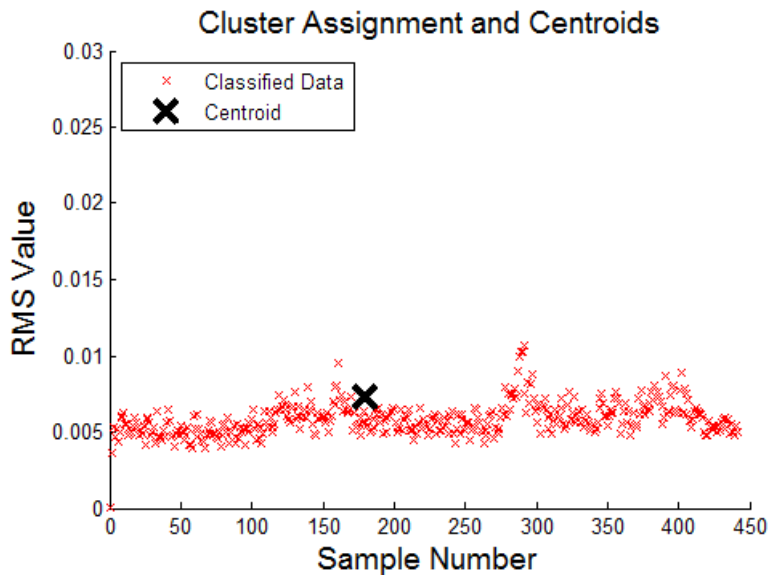


**Figure 5.6** K-Means clustering for machining data

PSO is used to train the feed forward neural network. The initial position and velocity of weights is initialized with random numbers between 0 and 1. The other parameter values used to train the neural network are tabulated in table 5.1.

**Table 5-1** Parameter values for PSO algorithm

Parameter	Value
$C_1, C_2$	2
$\omega$	2
$\omega_{max}$	0.9
$\omega_{min}$	0.5
$dt$	0.8
No. of Dimensions	Number of NN weights=61
Population size	70

As given in the table, population size for PSO algorithm is set to be 70, while the inertia weight is taken as 2 with maximum and minimum values as 0.9 and 0.5 respectively. Mean Square Error of the neural network is taken as the fitness function in the algorithm. The neural network is trained using the same dataset 'A' containing 881 sample points in which 441 samples are from machining signal and other 440 samples are from background machines. The neural network is trained for 100 iterations. Training curve of the neural network is shown in figure 5.7. It can be seen from the figure that the MSE of the neural network decreased sharply for forty iterations and then slope of the curve tends to become constant. However, the minimum value of the mean square error is found to be 0.2182 at 90<sup>th</sup> iteration.

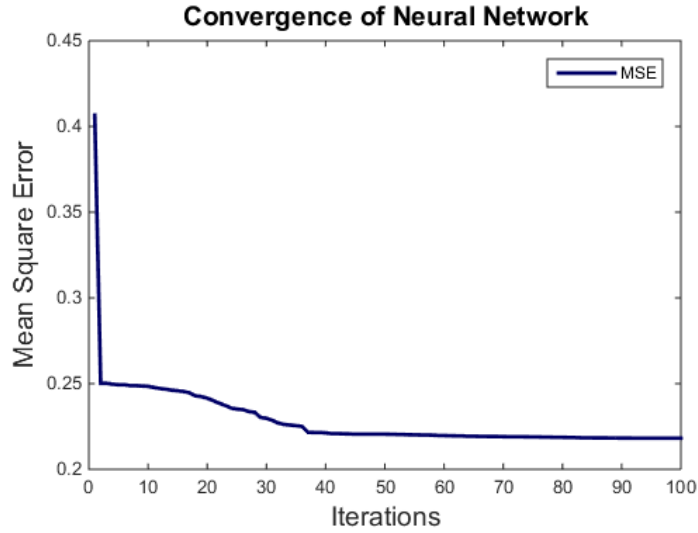


**Figure 5.7** Training curve of PSO neural network

To test the neural network, features from 1 sec data from each machine signal are fed to the neural network and its response is recorded. The confusion matrix of neural network response for the machining signal is shown in the figure 5.8.

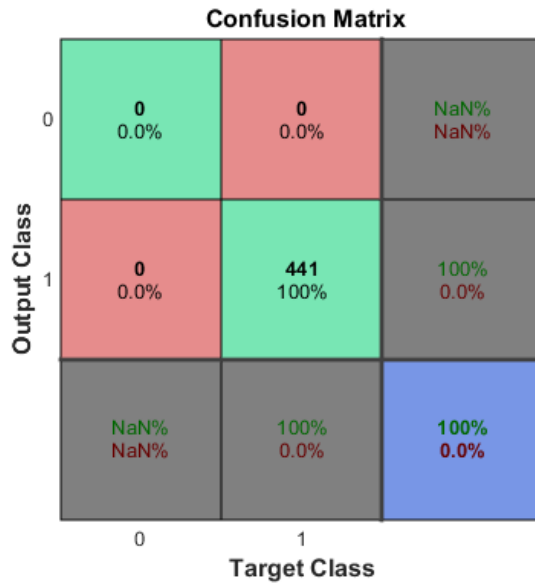


**Figure 5.8** Confusion matrix for PSO testing

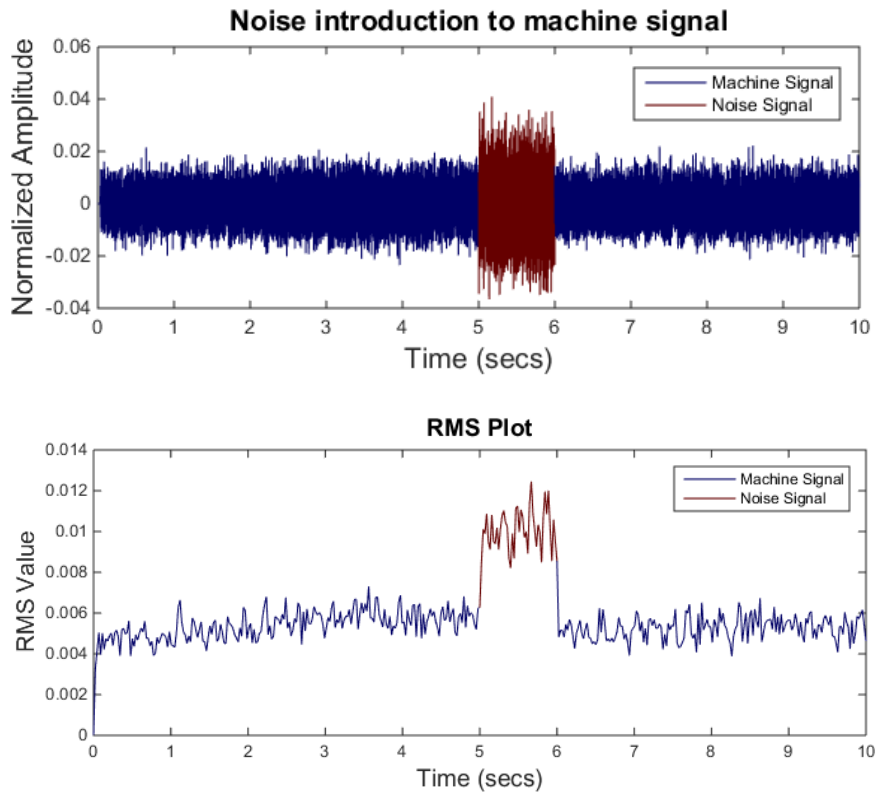
Results of all selected machine learning algorithms for dataset B is summarized in table 5.2.

**Table 5-2** Results Summary

	MC	M1	M2	M3	M4
<b>LM</b>	82.3	96.1	100	95.7	5
<b>SOM</b>	100	0	99.4	0	0
<b>Kmean</b>	100	0	99.5	0	0
<b>PSO</b>	100	0	99.7	0	0

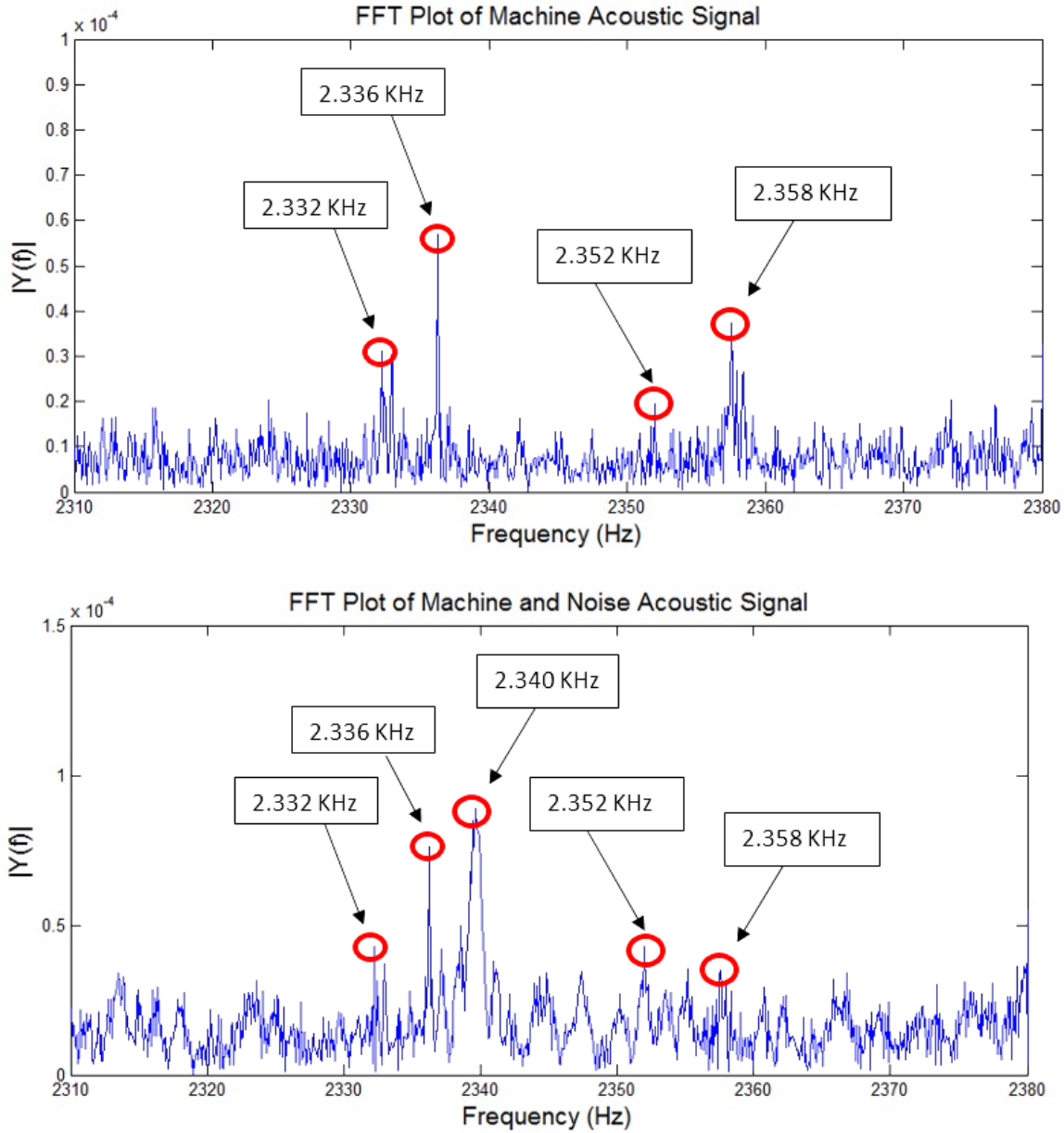
It can be seen that SOM, K-Mean and PSO trained neural network could classify only dominant noise, however, they could not classify the other noise. Back-propagation neural network shows better performance than other algorithms and it classified all types of noise, however, it fails for the M4 signal only. Therefore, back-propagation neural network is selected for further testing.

So far the back-propagation network is tested against individual signals. Now, the filtering efficiency of back-propagation network is tested for real scenario in which the actual machining signal is mixed with the background signal from different sources. For this purpose the background signals in different combinations are introduced to the machining signal for a window length of 1 sec. Figure 5.9 (a) shows a machining signal containing background signal of M4 for a period between 5 to 6 seconds. The RMS of the signal is then calculated as shown in figure 5.9(b). It can be seen that RMS level of signal between 5 to 6 seconds is higher than rest of the signal.



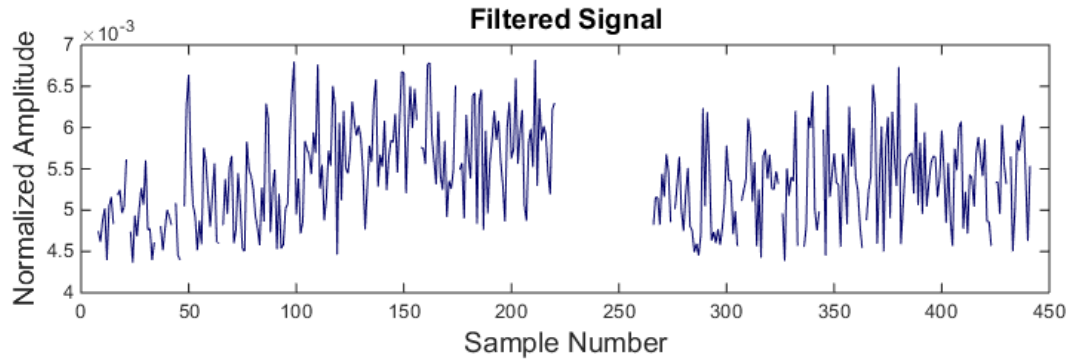
**Figure 5.9** Noise introduction (above) and RMS level of the same signal (below)

Figure 5.10 (a) shows the FFT plot of the signal before and after addition of the background noise then in addition to the dominant peaks at 2.332 kHz, 2.336 kHz, 2.352 kHz and 2.358 kHz (Figure 5.10(a)), there is an additional peak at 2.340 kHz is observed (Figure 5.10(b)). Moreover, the noise has also affected the amplitudes of the dominant frequencies as can be clearly seen from figure 5.10(b). As compared to figure 5.10 (a), figure 5.10(b) clearly indicates the dominant frequency from background signal. This in-turns proves the hypothesis that frequency based filtering technique cannot be applied as there is a chance of losing frequency of interest within range specified for airborne acoustic emission.



**Figure 5.10** FFT Plot of signal before and after addition of noise

The noisy signal is then passed through the back-propagation neural network. Figure 5.11 shows the filtered signal. It can be seen that RMS values between 220 and 264 sample numbers which corresponds to the noisy patch in the signal are filtered. However, some other values from the machining signal are also wrongly classified.



**Figure 5.11** Signal filtration using back-propagation neural network

## 5.2. Signal reconstruction

To reconstruct the filtered signal a time series model ARMA based algorithm is developed. In order to estimate order of the ARMA model, a minimum of 50 points are needed, therefore, to make the signal continuous or to reconstruct the filtered values for first 50 samples, the filtered values are initially replaced by average of the two neighbor samples.

Variance test has been used in order to check the stationarity of the signal. Variance of the signal is calculated and recorded for the series and then series is differenced until we found minimum variance. However, in our case, the variance is found to be minimum for order of different equal to 1. Therefore, one difference of the series is taken. Table 5-3 shows the different values of variance calculated at different order of difference. It can be seen that variance is minimum at D1.

**Table 5-3** Variance value at different order of difference

Order of difference	Variance
Variance	4.76e-07
D1	4.70e-07
D2	9.37e-07
D3	2.51e-06
D4	8.09e-06

ACF and PACF tests are used to calculate order of MA and AR models respectively. Figure 5.12 shows the ACF plot of the signal. ACF is calculated for 20 lags only. It can be seen that only one peak at the lower lags is above the upper bound of the graph. This is suggesting that MA model should be of order 1.

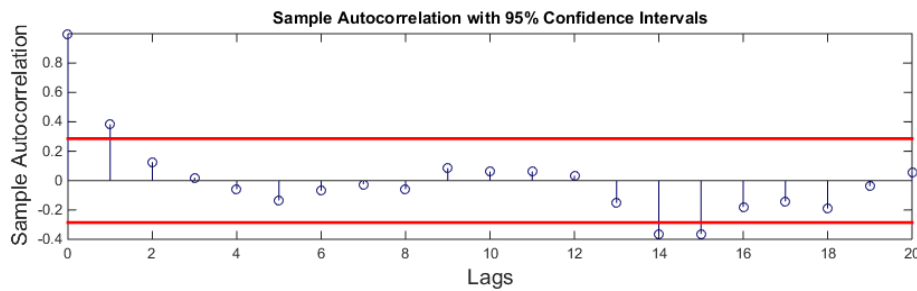


**Figure 5.12** ACF plot

Figure 5.13 shows the PACF plot of the signal which is also calculated for 20 lags only. A peak of 0.4 is found at lag 1 which is suggesting AR model of order 1. However, ARIMA models with  $p=1,2,3,4$  and  $q=1,2,3,4$  are also investigated and the best results are found are ARIMA (2,1,2).

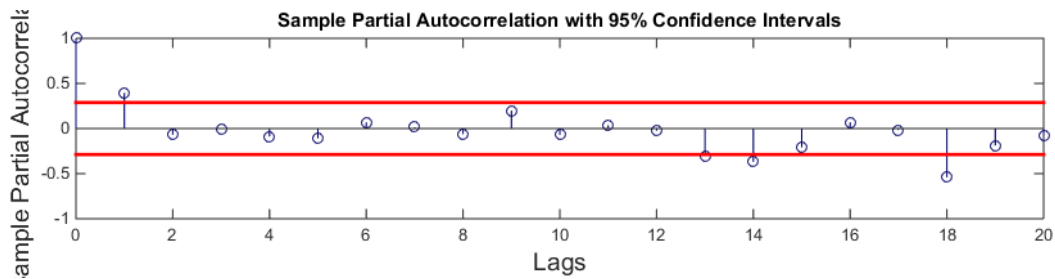


**Figure 5.13** PACF Plot

The coefficient values for the selected model is found using Maximum Likelihood Estimation. The values of the coefficients are tabulated in table 5-4.

**Table 5-4** Estimated coefficients values

Model	Coefficient 1	Coefficient 2
Autoregressive model ( $\emptyset$ )	-0.0186	0.6104
Moving Average model ( $\theta$ )	-0.1894	-0.8105

The estimated ARMA model is then used to reconstruct the filtered signal. A window of 50 samples is selected and then maximum of 5 samples are forecasted in order to reconstruct signal. Then window is moved to next 50 values of the signals and same procedure is repeated until complete signal is reconstructed. After that, filtered values for first 50 samples which were replaced by average of their neighbor samples, are now replaced by average of the filtered signal. Figure 5.15 shows the reconstructed signal.

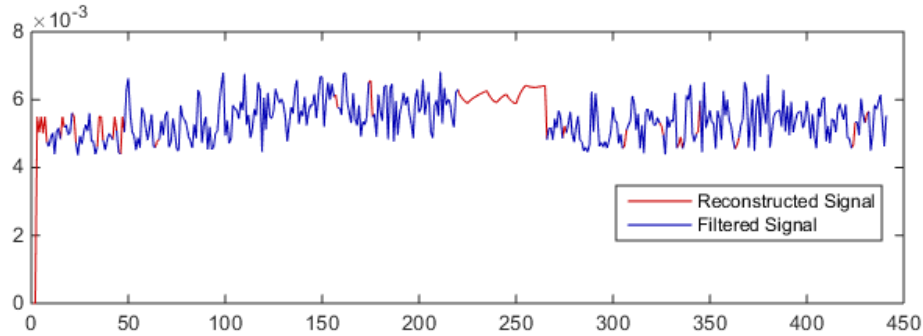


**Figure 5.14** Reconstructed Signal

In the above figure, machining signal is shown by blue line while the filtered or reconstructed samples are shown by red line. Table 5.4 shows the filtering results of back-propagation neural networks for machining signal containing different combinations of background noise. SNR1 depicts the signal-to-noise ratio before filtering, whereas, SNR2 shows the signal-to-noise ratio after filtering and reconstruction. Statistically, SNR is the ratio of mean value of the signal to its standard deviation. Mathematically it can be defined as

$$SNR = \frac{\bar{S}}{\sigma_s} = \frac{\frac{1}{N} \sum_{i=1}^N S_i}{\sqrt{\frac{1}{N} \sum_{i=1}^N (S_i - \bar{S})^2}}$$

where  $\bar{S}$  is mean value of signal and  $\sigma_s$  is standard deviation of signal.

Similarly, CV1 and CV2 are the coefficients of variation before and after filtering respectively. SNR and coefficient of variation are reciprocal of each other.

As it is clear from table 4 that SNR values for different combination of background noise with machine signal are improved after filtering and reconstruction. However, some of the contribution to this improvement in SNR is also due to false positives. On the other hand,

coefficient of variation (CV) decreases after filtering. Column 9 of the table shows the percentage increase in the SNR before and after filtering the noise.

**Table 5-5** Results for real scenarios

Noise	MEAN1	STD1	SNR1	CV1	MEAN2	STD2	SNR2	CV2	% inc
MC+M1	0.005812	0.001619	3.590631	0.278503	0.005447	0.000697	7.810309	0.128036	54.02703
MC+M2	0.010439	0.015243	0.684827	1.460222	0.005447	0.000697	7.810309	0.128036	91.23175
MC+M3	0.00551	0.000903	6.098895	0.163964	0.005478	0.000732	7.486404	0.133575	18.53372
MC+M4	0.005634	0.001161	4.851321	0.206129	0.005478	0.000729	7.513827	0.133088	35.43474
MC+M1+M2	0.010501	0.015425	0.680738	1.468993	0.005447	0.000697	7.810309	0.128036	91.28411
MC+M1+M3	0.00588	0.001809	3.250408	0.307654	0.005447	0.000697	7.810309	0.128036	58.38311
MC+M1+M4	0.005959	0.002025	2.943519	0.339729	0.005447	0.000697	7.810309	0.128036	62.31238
MC+M2+M3	0.010456	0.015291	0.683811	1.462392	0.005447	0.000697	7.810309	0.128036	91.24476
MC+M2+M4	0.010473	0.015351	0.682253	1.465732	0.005447	0.000697	7.810309	0.128036	91.26471
MC+M3+M4	0.005707	0.001345	4.242938	0.235686	0.005447	0.000697	7.810309	0.128036	45.67516
MC+M1+M2+M3	0.010519	0.015476	0.67967	1.471302	0.005447	0.000697	7.810309	0.128036	91.29778
MC+M1+M2+M4	0.010535	0.015532	0.678289	1.474298	0.005447	0.000697	7.810309	0.128036	91.31547
MC+M1+M3+M4	0.006018	0.002191	2.746179	0.364142	0.005447	0.000697	7.810309	0.128036	64.83905
MC+M2+M3+M4	0.010491	0.015397	0.68133	1.467718	0.005447	0.000697	7.810309	0.128036	91.27653
MC+ All Noise	0.010553	0.015581	0.67731	1.476429	0.005447	0.000697	7.810309	0.128036	91.328

MSE
1.34E-07
1.34E-07
1.68E-07
1.72E-07
1.34E-07

### 5.3. Summary

The chapter can be summarized as follows:

- ❖ Performance of different machine learning algorithms as adaptive filters has been tested under different conditions. Four different algorithms, back-propagation neural network from the supervised learning, Self-Organizing Map neural network (SOM) from the unsupervised learning, K-mean from clustering algorithms and Particle Swarm Optimization from the optimization algorithms have been selected in this regard.
- ❖ SOM neural network, K-Mean algorithm, and neural network trained with the PSO algorithm are able to classify M2 signal only because of its dominant nature. Back-propagation neural network shows better performance and filter all types of noise, however, it shows the worst performance in case of M4 due to its overlapping RMS with the machining signal.
- ❖ Back-propagation neural network is selected and further tested with noisy signals under real scenario in which the noise would be mixed with the machining signal. The neural network is able to classify all type of noise in this case, however, some machining signal samples are also miss-classified as noise signals.
- ❖ ARMA has never been used in the literature to reconstruct the signal for machining process. It shows promising results with average increase in SNR of 70.3% before and after signal reconstruction. Moreover, an average MSE of  $1.3 \times 10^{-7}$  is found between reconstructed and original machining signal.

## 6. CHALLENGES

Many researchers have used air-borne acoustic emission to monitor tool health. However, there are few challenges in implementation of the technique. One of the major challenges in implementation of the technique is the environmental noise such as sounds from parallel running machines, operator voice or sounds in background etc. This research tried to provide a solution to the earlier mentioned problem, however, there are various scenarios that can be a problem in real implementation of the proposed technique.

The other type of noise such as noise from the process itself, noise from other parts of the machine such as spindle noise, door opening and closing etc., are still a problem for the proposed technique and must be catered. Noise from the surrounding environment has a great variability and may vary from operator talking, to a ringing bell in the background, thus, may pose a serious challenge to the technique. Moreover, the technique would be environment specific, i.e., during the installation of the CNC machine on a job floor, neural network has to be trained with the environmental noise for a data consisting of noise of the floor. In this case, another challenge would be the installation of a new machine in the surrounding environment. In order to filter the noise of known frequencies such as the noise of door opening and closing, notch filter of known frequency can be used. To filter the noise of variable frequency, a number of mics can be installed at different locations in the workplace in order to detect the noise frequencies and to filter them from the machining signal.

Another challenge to the proposed technique is the variability of the machining signal RMS. Results are calculated for a specific RMS level of the machining signal, however, this RMS level increases with increase in the tool degradation. Hence, RMS level of the machining signal is variable, therefore, response of the neural network will be different for different machines. For

example, it may be possible that at time  $t$ , RMS level of a background machine is higher than the machining signal. However, with the increase in RMS level of the machining signal at time  $t+1$ , that machine can have overlapping RMS with machining signal, therefore, the neural network would confuse background noise with the machining signal and would not filter it out. . In order to overcome the problem of variability of RMS of the machining signal, some other features such as kurtosis, skewness, etc., can be used.

A challenge to reconstruct the filtered signal would be in the case that if the surrounding machines are running prior to the machining process begin. In this case, the starting values of the signal will be filtered and therefore, ARMA would have to back cast the signal, instead of forecast, to reconstruct the signal. In order to develop the signal reconstruction algorithm, only one second noise is introduced to the machining signal between 5 and 6 sec. However, in real scenario, length of the noise may equal to signal length. In this case, complete signal will be filtered out by neural network. The proposed technique requires at least 50 samples of the pure machine signal in order to estimate the ARMA model to reconstruct the signal. The 50 samples represents 1.1 sec data approximately.

## 6.1. Summary

The chapter can be summarized as follows

- ❖ There are various challenges in implementation of the proposed technique. Different type of environmental noise can disturb machining signal. Some noise which lie outside the machining frequency range, can be filtered using notch or traditional filters.
- ❖ The proposed technique would be environment specific, i.e., the system needs to learn about the environment acoustics of the floor before it can predict tool health. Variable RMS of machining signal as well as of noise could pose a challenge to the proposed technique.

- ❖ In order to reconstruct the filtered signal using ARMA based algorithm, at least 50 samples of pure machining signal is required to determine the order of ARMA model.

## 7. CONCLUSION AND FUTURE WORK

Airborne acoustic emission from a machining process provides a vital information regarding the tool wear and can be used to develop a low-cost solution to monitor tool health. However, background noise is one of major challenge in its implementation. The aim of the research is to propose a solution to filter the noise generated by parallel running machines on the shop floor in order to overcome implementation challenge of air-borne acoustic emission in industrial environment. Characteristic frequency of tool condition for air-borne acoustic emission lies within first few KHz. Parallel running machining machines frequency can lie within or outside this range. Traditional band-pass, band-stop or notch filters can be applied if noise frequency lies outside the machining frequency range, however, these filters would also filter the machining signal if the noise frequency lies within the machining frequency range. Therefore, different techniques of machine learning algorithms have been used as adaptive filters to classify machine and noise signals.

Four different algorithms, back-propagation neural network from the supervised learning, Self-Organizing Map neural network (SOM) from the unsupervised learning, K-mean from clustering algorithms and Particle Swarm Optimization from the optimization algorithms have been investigated. The selected techniques adapt themselves according to environmental conditions and extract the machining signal from background noise effectively. SOM neural network, K-Mean algorithm, and neural network trained with the PSO algorithm are able to classify grinding machine signals as the signal was quite distinct from the machining signal, and show accuracy of 99.4%, 99.5%, and 99.7% for grinding machine signal respectively. One of the possible reason for high accuracy is distinctiveness of the grinding machine signal from the machining signal. These algorithms are not able to classify other noise signals. Back-propagation neural network shows better performance and filter all types of noise. It shows the best performance for grinding machine with an accuracy of 100%. The accuracies for variable speed DC motor, 3-axis milling machine and machining signal are found to be 96.1%, 95.7% and 82.3% respectively. The accuracy is determined

to be minimum at 5% in case of 4 axis mini milling machine. The reason for the worst performance of back-propagation neural network in case of 4-axis mini milling machine is the overlapping RMS level of the signal with machining signal. Hence, backpropagation is found to be a suitable candidate to filter background noise, as it works for all background machines noise.

Different combinations of noise signals are mixed and introduced to machine signal in order to test the performance of proposed solution in real environment. To reconstruct the filtered signal, ARMA based algorithm is used. A series needs to be stationary to estimate the ARMA model. Proper order of differencing is selected using variance and autocorrelation function in order to avoid under and over differencing of the series. An under-differenced would behave as non-stationary series, while on the other hand, it is difficult to estimate over-differenced series coefficients. Order of moving average and autoregressive model are estimated to be around 1 using autocorrelation and partial autocorrelation function test, however, better results are found at ARIMA (2, 1, 2). ARMA based signal reconstruction shows promising results with average increase in SNR of 70.3% before and after signal reconstruction. Moreover, an average MSE of  $1.3 \times 10^{-7}$  is found between reconstructed and original machining signal.

Finally, it can be concluded that the proposed technique can work best for lab environment, however, the proposed technique can face a challenge to filter the noise having characteristics closer to machining signal. Moreover, implementation of ARMA based reconstruction algorithm in the dominant noisy environment would be a challenging problem.

Future aim of the research is to explore the suitable techniques and methods to overcome the challenges mentioned in chapter 6. This may involve analysis of environmental noise in order to filter it out eventually. Noise can be recorded for a particular duration at regular intervals for the whole day in this regard. This data can be used to train the neural network to adapt the algorithm to environment. Future work also involves analysis of variability of noise signal, so that all type of parallel running machine noise can be filtered. Different features from the signals can be used along with the already used features. Signal reconstruction algorithm must be made more robust so that it can work for all scenarios as mentioned in chapter 6. Future work may also involve investigation of various algorithms to filter out the background noise. These algorithms may include Markov Models.

Currently, neural network performance is optimized using PSO algorithm. In future, Genetic Algorithms can also be used in order to optimize the neural network weights. Blind source separation using a single or two microphones can be done to extract the machining signal from mixed signal instead of filtering out the noise.

## 7.1. Summary

The chapter can be summarized as follows

- ❖ In order to filter parallel running machines noise from machining signal, machine learning algorithms have been used as adaptive filters. Among the four machine learning algorithms, back-propagation neural network showed better performance.
  
- ❖ A novel ARMA based algorithm has been developed to reconstruct the filtered signal. In order to make series stationary, proper order of the differencing must be selected through variance and ACF tests. Order of ARMA model can be selected using ACF and PACF tests whereas, model coefficients can be estimated through Maximum Likelihood Estimation method.
  
- ❖ Future work include to analyze and then propose solution to the challenges discussed in chapter 6. It also includes study of various other algorithms to improve the performance of proposed technique.

## REFERENCES

- [1] "Manufacturing, value added (current US\$)," World's Bank, 2011. [Online]. Available: <http://databank.worldbank.org/data/views/reports/metadataview.aspx>. [Accessed 16 June 2015].
- [2] A. G. Reborn, J. Jiang and P. E. Orban, "State-of-the-art methods and results in tool condition monitoring: a review," *The International Journal of Advanced Manufacturing Technology*, vol. 26, no. 7- 8, pp. 693-710, 2005.
- [3] R. Thomson, M. Edwards, E. B. Ton and B. Rabenau, "Predictive maintenance, Is the timing right for predictive maintenance in the manufacturing sector?," Roland Berger, 2014.
- [4] "AIMACS," 2013. [Online]. Available: <http://www.aimacs.eu/about.html>. [Accessed 17 May 2015].
- [5] Y. M. Zhang, *Real-Time Weld Process Monitoring*, Elsevier, 2008.
- [6] M.-C. Lu and E. Kannatey-Asibu, "Flank Wear and Process Characteristic Effect on System Dynamics in Turning," *Journal of Manufacturing Science and Engineering*, vol. 126, pp. 131-140, 2004.
- [7] D. Mba and J. Z. Sikorska, "Challenges and obstacles in the application of acoustic emission to process machinery," *Part E: J. Process Mechanical Engineering*, vol. 222, no. 1, pp. 1-19, 2008.
- [8] M. Sortino, "Application of statistical filtering for optical detection of tool wear," *International Journal of Machine Tools & Manufacture* , vol. 43, p. 493–497, 2003.
- [9] S. Kurada and C. Bradley, "A review of machine vision sensors for tool condition monitoring," *Computers in Industry*, vol. 34, pp. 55-72, 1997.
- [10] S. Dutta, S. Pal, S. Mukhopadhyay and R. Sen, "Application of digital image processing in tool condition monitoring: A review," *CIRP Journal of Manufacturing Science and Technology*, 2003.
- [11] X. Li, "Real-time tool wear condition monitoring in turning," *International Journal of Production Research*, vol. 39, no. 5, pp. 981-992, 2001.
- [12] M. Ahmad, M. Nuawia, S. Abdullah, Z. Wahid, Z. Karim and M. Dirhamsyah, "Development of tool wear machining monitoring using novel statistical analysis method, I-kaz," *Procedia Engineering*, vol. 101, p. 355 – 362, 2015.
- [13] H. Chelladurai, V. K. Jain and N. S. Vyas, "Development of a cutting tool condition

- monitoring system for high speed turning operation by vibration and strain analysis," *Int J Adv Manuf Technol*, vol. 37, p. 471–485, 2008.
- [14] D. Cotterell and M. O’Sullivan, "Temperature sensing in single point turning," *Journal of material processing technology*, vol. 118, pp. 301-308, 2001.
- [15] N. Ghosh and e. al., "Estimation of tool wear during CNC milling using neural network-based sensor fusion," *Mechanical Systems and Signal Processing*, vol. 21, no. 1, pp. 466-479, 2007.
- [16] T. Segreto, A. Simeone and R. Teti, "Multiple sensor monitoring in nickel alloy turning for tool wear assessment via sensor fusion," *Procedia CIRP*, vol. 12, p. 85 – 90, 2013.
- [17] M. S. H. Bhuiyan, I. A. Choudhury and N. Yusoff, "A new approach to investigate tool condition using dummy tool holder and sensor setup," *Int J Adv Manuf Technol*, vol. 61, p. 465–479, 2012.
- [18] A. Hase, M. Wada, T. Koga and H. Mishina, "The relationship between acoustic emission signals and cutting phenomena in turning process," *Int J Adv Manuf Technol* , vol. 70, p. 947–955, 2014.
- [19] X. Li, "A brief review: acoustic emission method for tool wear monitoring during turning," *International Journal of Machine Tools & Manufacture*, vol. 42, pp. 157-165, 2002.
- [20] J. Kopac and S. Sali, "Tool wear during the turning process," *Journal of material processing technology*, vol. 113, pp. 312-316, 2001.
- [21] W. S. L. C. V. J. Emerson Raja, "Emitted Sound Analysis for Tool Flank Wear Monitoring using Hilbert Huang Transform," *International Journal of Computer and Electrical Engineering*, vol. 4 , no. 2, pp. 110-114, 2012.
- [22] B. P. Hede, "Condition monitoring of tools in CNC turning," Loughborough University, 2008.
- [23] G. Jang and T. Lee, "A Probabilistic Approach to Single Channel Blind Signal Separation".
- [24] C. Ruiz-Ca’rcel, E. Hernani-Ros, Y. Cao and D. Mba, "Use of Spectral Kurtosis for Improving Signal to Noise Ratio of Acoustic Emission Signal from Defective Bearings," *J Fail. Anal. and Preven.*, vol. 14, p. 363–371, 2014.
- [25] L. Zhang, Y. Shi, Z. Pang and L. Ren, "Adaptive Cancellation of Background Machine Noise Based on Combination of ICA-R and RBFNN," in *8th International Conference on Natural Computation*, 2012.
- [26] M. Z. Nuawi, F. R. Lamin, A. Ismail, S. Abdullah and W. Z., "A Novel Machining Signal Filtering Technique: Z-notch Filter, (2009)," *World Academy of Science, Engineering and*

*Technology*,, vol. 3, no. 6, 2009.

- [27] M. Senthilkumar, M. Vikram and B. Pradeep, "Vibration Monitoring for Defect Diagnosis on a Machine Tool: A Comprehensive Case Study," *International Journal of Acoustics and Vibration*,, vol. 20, no. 1, pp. 4-9, 2015.
- [28] J. C. Emmanuel, R. Justin and T. Terence, "Robust Uncertainty Principles: Exact Signal Reconstruction From Highly Incomplete Frequency Information," *IEEE TRANSACTIONS ON INFORMATION THEORY*,, vol. 52, no. 2, pp. 489-509, 2006.
- [29] A. Ukte, A. Kizilkaya and M. D. Elbi, "Statistical Multirate High-Resolution Signal Reconstruction Using The Empirical Mode Decomposition Based Denoising Approach," 2014.
- [30] P. Baraldi, F. DiMaio, P. Turati and E. Zio, "Robust signal reconstruction for condition monitoring of industrial components via a modified Auto Associative Kernel Regression method," *Mechanical Systems and Signal Processing*, vol. 60, no. 61, p. 29–44, 2015.
- [31] X. Chuangwen, L. Zhe and L. Wencui, "A frequency band energy analysis of vibration signals for tool condition monitoring," in *International Conference on Measuring Technology and Mechatronics Automation*, 2009.
- [32] M. Basri and et al, "Comparison of estimation capabilities of response surface methodology (RSM) with artificial neural network (ANN) in lipase-catalyzed synthesis of palm-based wax ester.," *BMC biotechnology*, vol. 7, no. 1, 2007.
- [33] "SDL Component Suite – Kohonen," [Online]. Available: <http://www.lohninger.com/kohonen.html>. [Accessed 29 January 2015].
- [34] T. Zafar, K. Kamal, R. Kumar, Z. Sheikh, S. Mathavan and U. Ali, "Tool Health Monitoring using Airborne Acoustic Emission and a PSO-optimized Neural Network," in *2nd IEEE Conference on Cybernetics*,, Gydnia, 2015.
- [35] S. Mirjalili and S. Z. M. Hashim, "A New Hybrid PSOGSA Algorithm for Function Optimization,," in *International Conference on Computer and Information Application ICCIA*, 2010.
- [36] G. E. P. Box, G. M. Jenkins and G. C. Reinsel, *Time Series Analysis: Forecasting and Control*,, NJ: Prentice Hall,, 1994.
- [37] W. H. Lavery, "Lecture Notes on ARMA," [Online]. Available: [math.usask.ca/~lavery/S349/S349Lectures/S349%2008.ppt](http://math.usask.ca/~lavery/S349/S349Lectures/S349%2008.ppt). [Accessed 6 March 2015].
- [38] MathWorks, "Matlab Help, Autocorrelation Function," [Online]. Available: <http://www.mathworks.com/help/econ/autocorr.html>. [Accessed 4 Feb 2015].

- [39] Mathworks, "Matlab Help, Sample Partial AutoCorrelation," [Online]. Available: [www.mathworks.com/help/econ/parcorr.html](http://www.mathworks.com/help/econ/parcorr.html). [Accessed 4 Feb 2015].
- [40] A. Brandt, Noise and vibration analysis: signal analysis and experimental procedures, John Wiley & Sons, 2011.
- [41] R. J. Boness, S. L. McBride and M. Sobczyk, "Wear studies using acoustic emission techniques," *Tribology international*, vol. 23, no. 5, pp. 291-295, 1990.
- [42] J. Barry, G. Byrne and D. Lennon, "Observations on chip formation and acoustic emission in machining Ti-6Al-4V alloy.," *International Journal of Machine Tools and Manufacture*, vol. 41, no. 7, pp. 1055-1070, 2001.
- [43] D. E. Lee, *et al*, "Precision manufacturing process monitoring with acoustic emission.," *International Journal of Machine Tools and Manufacture*, vol. 46, no. 2, pp. 176-188, 2006.
- [44] S. S. Cho and K. Komvopoulos, "Correlation between acoustic emission and wear of multi-layer ceramic coated carbide tools," *Journal of manufacturing science and engineering*, vol. 119, no. 2, pp. 238-246, 1997.



### **Completion Certificate**

It is to certify that the thesis titled“Background Noise Reduction and Signal Reconstruction for Airborne Acoustic Emission of a Machining Process”submitted by registration no. 2013NUST62510MCEME35513F, NS Tayyab Zafar of MS-78 Mechatronics Engineering iscomplete in all respects as per the requirements of MainOffice, NUST (Exam branch).

Supervisor: \_\_\_\_\_

Dr. Khurram Kamal

Date: \_\_\_\_ July, 2015